

Theses - Daytona Beach

Dissertations and Theses

4-1989

Data Reduction Procedure for an Experimental Method of Measuring the Velocity-Coupled Response Function of Solid Propellants

William H. Jarvis

Embry-Riddle Aeronautical University - Daytona Beach

Follow this and additional works at: <https://commons.erau.edu/db-theses>



Part of the [Aerospace Engineering Commons](#), and the [Computer Sciences Commons](#)

Scholarly Commons Citation

Jarvis, William H., "Data Reduction Procedure for an Experimental Method of Measuring the Velocity-Coupled Response Function of Solid Propellants" (1989). *Theses - Daytona Beach*. 101.
<https://commons.erau.edu/db-theses/101>

This thesis is brought to you for free and open access by Embry-Riddle Aeronautical University – Daytona Beach at ERAU Scholarly Commons. It has been accepted for inclusion in the Theses - Daytona Beach collection by an authorized administrator of ERAU Scholarly Commons. For more information, please contact commons@erau.edu.

NOTE TO USERS

**Page(s) not included in the original manuscript are
unavailable from the author or university. The
manuscript was microfilmed as received**

62

This reproduction is the best copy available.

UMI[®]

A THESIS
SUBMITTED IN PARTIAL FULFILLMENT OF THE REQUIREMENTS
FOR THE DEGREE OF
MASTER OF SCIENCE IN AERONAUTICAL ENGINEERING

DATA REDUCTION PROCEDURE FOR AN EXPERIMENTAL METHOD
OF MEASURING THE VELOCITY-COUPLED RESPONSE
FUNCTION OF SOLID PROPELLANTS

William H. Jarvis

Department of Aerospace Engineering
Embry Riddle Aeronautical University

April 1989
Advisor: Prof. L.L. Narayanaswami

UMI Number: EP31843

INFORMATION TO USERS

The quality of this reproduction is dependent upon the quality of the copy submitted. Broken or indistinct print, colored or poor quality illustrations and photographs, print bleed-through, substandard margins, and improper alignment can adversely affect reproduction.

In the unlikely event that the author did not send a complete manuscript and there are missing pages, these will be noted. Also, if unauthorized copyright material had to be removed, a note will indicate the deletion.



UMI Microform EP31843
Copyright 2011 by ProQuest LLC
All rights reserved. This microform edition is protected against
unauthorized copying under Title 17, United States Code.

ProQuest LLC
789 East Eisenhower Parkway
P.O. Box 1346
Ann Arbor, MI 48106-1346

DATA REDUCTION PROCEDURE FOR AN EXPERIMENTAL METHOD
OF MEASURING THE VELOCITY-COUPLED RESPONSE
FUNCTION OF SOLID PROPELLANTS

by

William H. Jarvis

This thesis was prepared under the direction of the candidate's thesis committee chairman, Dr. L.L. Narayanaswami, Department of Aeronautical Engineering, and has been approved by the members of his thesis committee. It was submitted to the School of Graduate Studies and Research and was accepted in partial fulfillment of the requirements for the degree of Master of Science in Aeronautical Engineering.

Thesis Committee:

Dr. L.L. Narayanaswami, May 2, 1989
Dr. L.L. Narayanaswami

Dr. W.P. Schimmel
Dr. W.P. Schimmel

T.R. Gupta 5/8/89
Dr. T.R. Gupta

Howard D. Lentz, Jr., J.G. Ladewig
Program Coordinator
Howard D. Lentz
Department Chair

Dean, School of Graduate Studies and Research

Date

Acknowledgment

The author wishes to thank Professor L.L. Narayanaswami for his assistance in formulating the objective of this work and for his expert guidance throughout the investigation.

The author also wishes to thank Professor W.P. Schimmel and Professor T.R. Gupta for their critical review of the thesis and useful suggestions.

Special thanks must go to Professor S.S. Dalal for supporting and encouraging my presentation of a portion of this material at the twenty-second annual meeting of the Mathematical Association of America in Gainesville, Florida.

Abstract

Author: William H. Jarvis

Title: Data Reduction Procedure for an Experimental Method of Measuring
the Velocity-Coupled Response Function of Solid Propellants

Institution: Embry-Riddle Aeronautical University

Degree: Master of Science in Aeronautical Engineering

Year: 1989

A computer program has been developed for calculation
of the velocity-coupled response function of solid-
propellants from experimentally measured pressure data.

The proposed velocity-coupled response function measurement
apparatus consists of an end-burner combustor where the
propellant sample is oscillated in a direction normal to the
flow in the presence of a standing acoustic wave within the
combustion chamber. The pressure measurements are made at
select points along the length of the chamber.

The data reduction program consists of a Runge-Kutta
routine driven by a BFGS multivariable search routine. The
Runge-Kutta routine determines the pressure distribution
within the chamber of the proposed apparatus for a specific
velocity-coupled response function (R_v). The BFGS
optimization routine searches for the R_v which minimizes the
difference between the calculated and measured
pressure distributions.

The data reduction program has demonstrated convergence
to the proper R_v value for pressure data that was generated
by sampling from gaussian distributions.

Table of Contents

	Page
Acknowledgment	iii
Abstract	iv
List of Symbols	vi
1.0 Introduction	1
2.0 Historical Background	3
3.0 New Method	8
4.0 Data Reduction Procedure	10
5.0 Numerical Solution of Governing Equations	13
5.1 Governing Equations	13
5.2 Boundary Conditions	17
5.3 Temperature Distribution	18
6.0 Error Function	19
7.0 Location of Pressure Ports	21
8.0 Optimization Procedure	22
8.1 BFGS Algorithm	22
8.2 Fibonacci Line Search	24
9.0 Description of Computer Program	29
9.1 Admittance to Velocity-Coupled Response Function Conversion	29
9.2 Runge-Kutta Algorithm	30
9.3 BFGS Search Algorithm	31
10.0 Simulation of Experiment	33
11.0 Simulation Results	34
12.0 Conclusion	48
13.0 Recommendations for Future Work	49
References	50
Appendices	52

Symbols

u_n - velocity of flow normal to the propellant
 p - pressure
 ρ - density
 T - temperature
 a - acoustic velocity
 u'_e - average relative velocity of propellant sample
 $(\bar{})$ - mean flow quantity
 (δ) - perturbation flow quantity
 R_v - velocity-coupled response function
 R_p - pressure-coupled response function
 i - square root of negative one
 ω - angular frequency
 α - growth constant, parameter in linear equation
 p'_m - measured perturbation pressure
 p'_n - numerically calculated perturbation pressure
 E - least squares error function
 k_c - conductivity of combustion product
 k_z - conductivity of chamber wall
 r - radius of combustion chamber
 L - length of combustion chamber
 T_∞ - ambient temperature
 Δt - thickness of chamber wall
 \bar{M} - mean flow Mach number
 λ - equal to $2 \frac{k_z}{k_c} \frac{1}{r \Delta t}$
 x - coordinate direction along axis of combustion chamber

1.0 Introduction

From the beginning of solid propellant rocket development, the rocket engine designer has been troubled by the phenomenon broadly described as "unstable combustion". Normal combustion of a solid propellant is defined as the regular predictable process associated with steady conditions. Under steady conditions the burning rate of the propellant depends on the local mean pressure and the local mean mass flow moving parallel to the burning surface, and the initial propellant temperature. With the exceptions of detonations and explosions, unstable combustion in any combustion process is undesirable.

It is important to distinguish between two aspects of unstable combustion: irregular combustion refers to combustion associated with large deviations in the mean burning rate from that predicted under steady conditions while oscillatory combustion refers to combustion with periodic variations in flow properties about their mean values.

Oscillatory combustion instabilities arise from the coupling of pressure and velocity perturbations that are associated with the presence of acoustic modes within the combustion chamber, with the combustion processes in the burning zone at the solid propellant surface.

It is customary to assume that the fluctuation in the mass flow can be separated into a pressure-coupled part and a velocity-coupled part which are independent of each other.

Accordingly, the effects of pressure and velocity perturbations on the burn rate can be represented by the following equation (Ref. 1).

$$\frac{\dot{m}_e'}{\dot{m}_e} = R_p \frac{R'}{\delta \rho} + R_v \frac{\dot{w}_e'}{\dot{a}} \quad (1.1)$$

Since the solid propellant combustion responses, R_p and R_v , are the sources of acoustic amplification, their accurate determination is required for a complete stability analysis. Due to the complicated nature of the combustion process, it is difficult to predict the burn rate of a solid propellant on the basis of its chemical properties alone. For this reason, researchers have relied heavily on experimental approaches to combustion response function prediction. At the present time, methods to measure the combustion responses are being developed.

This investigation will focus on the data reduction procedure for a new method of experimentally measuring the velocity-coupled response function.

2.0 Historical Background

At the present time, a theoretical analysis of combustion instability containing all relevant parameters does not exist. This is largely because of an incomplete understanding of the response of the propellant burning rate to oscillations in the pressure and velocity of the flow adjacent to the propellant surface. Satisfactory models and reliable experimental techniques to predict the velocity-coupled response functions of solid propellants have remained particularly elusive. Until further progress is made in our understanding of the mechanistic basis for velocity coupling, research must be directed towards the development of experimental techniques for the measurement of the velocity-coupled response function. Solution to the problem of velocity-coupled response function measurement will be adequate only when there is quantitative agreement between the various experimental methods and realistic analytical models.

The measurement of combustion response functions has been attempted by a variety of methods, each having its advantages and shortcomings. The methods are best categorized by the type of burner used in the measurement and by the nature of the exciting disturbance. Burner configurations which have been used in the past include the center-vented burner, the modulated exhaust flow burner, the impedance tube burner and the bulk-mode self-excited burner. Acoustic oscillations in the burners are either self-excited

or generated by external means. The center-vented burner, commonly referred to as the T-burner, is an example of a self-excited burner. The rotating-valve method is an example of a burner where the oscillations are generated by external means. The T-burner and the rotating-valve methods deserve particular attention not only because of their extensive use and evaluation, but also because they are helpful in understanding the basic approach to experimental combustion response measurement.

The simplest form of the T-burner (Ref. 2) for pressure-coupled response measurements consists of a circular tube with propellant disks mounted at both ends. The products of combustion are exhausted through a vent at the center of the tube. This configuration allows maximum excitation of the fundamental longitudinal acoustic mode in the tube, thereby generating maximum acoustic pressures at the burning propellant surfaces. By placing the exhaust vent at the center of the tube where the pressure oscillations have the lowest amplitude, energy losses from the acoustic field are minimized. The exhaust vent is usually connected to a surge tank which is pressurized with nitrogen to the desired mean pressure. When the propellant disks are ignited, the propellant reaction flushes out the inert nitrogen, and oscillations develop and grow exponentially until losses limit the amplitude. When the propellant burns out, the oscillations decay in a roughly exponential manner. In its simplest use, it is assumed that the damping is the

same during the period of growing oscillations as during the period of decaying oscillations. The initial growth constant of the acoustic field (\propto) can then be regarded as the difference between the energy gains and the measured damping contribution, hence

$$\propto = \alpha_{\text{gain}} - \alpha_{\text{damp}} \quad (2.1)$$

Using linear acoustic theory, the rate at which energy is transferred to the acoustic field can be related to the response function. For end-burners the relation between and the pressure-coupled response is given by

$$\alpha_{\text{gain}} = 4f(\bar{M}_b R_p) \quad (2.2)$$

where f is the frequency of the oscillating field and \bar{M}_b is the mean flow Mach number. Using equations (2-1) and (2-2), the response function can be inferred from measurements of the growth constant and the damping constant.

Measurement of the velocity-coupled response function is much more difficult than measurement of the pressure-coupled response function. However, methods for adapting the T-burner for velocity-coupled measurements have been considered. In order to induce velocity-coupled response, the propellant test sample is exposed to a parallel velocity flow in locations which maximize velocity-coupled acoustic excitations. One means of accomplishing this is to mount the test charges on the side walls and the driver propellant at the ends. The difficulty with this arrangement is that test samples respond to both pressure and velocity oscillations. Hence, independent information about the

pressure-coupled response is required before the velocity-coupled contribution can be extracted from the measured pressure data. Variable-area methods with the propellant samples located at the L/4 and 3L/4 positions along the tube have also been considered. The basis for the variable-area method becomes clear if we extend equation (2.1) to the case where the propellant surface area is not equal to the cross-sectional area of the burner tube. Equation (2.1) becomes

$$\alpha = \alpha_{\text{gain}} \left(\frac{S_b}{S_c} \right) - \alpha_{\text{loss}} \quad (2.3)$$

which is the equation of a straight line for α with the area ratio as the dependent variable. The energy constant (α_{gain}) is the slope of this line. From the energy constant the real part of the response function can be determined. The primary disadvantage of variable-area methods is that several tests must be conducted to obtain the response function at a specific frequency and pressure. Other disadvantages include the theoretical uncertainties that are not reflected in the simplified expression for α in equation (2.1).

The basic approach to rotating-valve methods (Ref. 3) is to use exhaust modulation to control the acoustic oscillations in the combustion chamber. The usual burner configuration is a rocket motor with a cylindrical mounted charge and a conventional nozzle to control the mean combustion pressure. A secondary orifice is operated periodically to produce oscillations at a desired frequency. For velocity-coupled response measurements, two rotating

valves are required. With one valve positioned at either end of the combustion chamber and oscillated directly out of phase, controlled velocity oscillations can be generated. Analytical solutions of the mass, momentum and energy equations for the rotating-valve burner configuration along with measured acoustic response data are then used to predict the velocity-coupled response function. Unlike the T-burner method, the rotating valve approach determines both the real and imaginary components of the response function.

Direct measurement of the oscillatory burning surface regression using microwaves has also been considered. This approach provides both magnitude and phase information about the combustion response functions without having to indirectly calculate them from measured acoustic data. However, the difficulty of isolating pressure-coupled contributions from the velocity-coupled contributions has not been resolved.

At present there is a lack of qualitative agreement among the different approaches, and it is difficult to ascertain which method is the best. Accuracy, cost and repeatability are criteria for the evaluation of their relative merits.

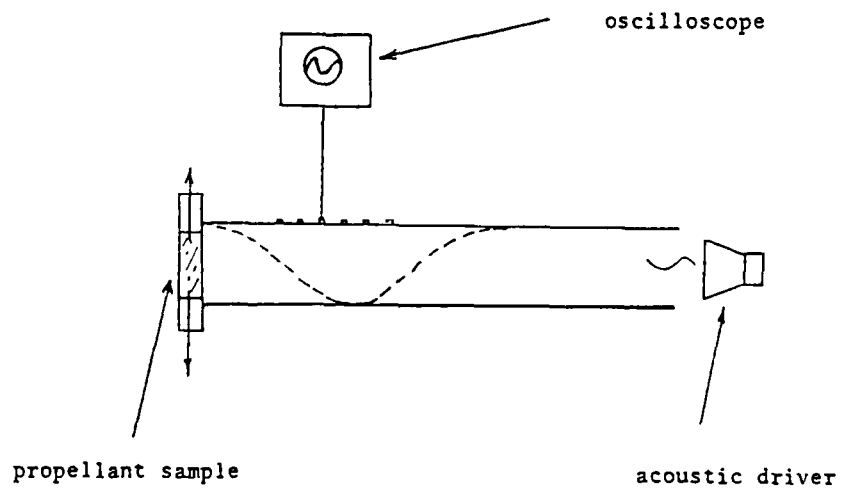
3.0 New Method

In a new attempt to determine the velocity-coupled response function from pressure oscillation data, L.L. Narayanaswami has suggested an end-burner test configuration where the propellant sample is oscillated normal to the flow in the presence of a standing acoustic wave in the combustion chamber (see Fig. 3.1).

Pressure coupling between the propellant burn rate and the acoustic field is generated by the oscillating pressure at the propellant surface. Velocity coupling is generated by relative flow oscillating tangential to the oscillating propellant surface.

The configuration of the standing wave within the combustion chamber is that of a forced standing wave in a closed-end tube modified slightly by the existence of pressure and velocity coupling between the propellant burn rate and the acoustic field. For given propellant sample, environmental conditions, and acoustic frequency, the configuration of the standing wave is uniquely determined by the combustion response functions R_p and R_v . The pressure-coupled response function (R_p) will be known from prior experiment and the velocity-coupled response function will be determined from pressure measurements along the length of the experimental device. This investigation will focus on the calculation of R_v from the pressure measurement data.

Figure 3.1 Schematic of Rv-Measurement Apparatus



4.0 Data Reduction Procedure

The data reduction procedure that was developed for the calculation of the velocity-coupled response function from experimentally measured pressure data is presented here. The prime motivation for the data reduction procedure is the lack of an accurate means for direct measurement of the perturbation velocity at the propellant surface.

An expression for the velocity-coupled response function is obtained from equation (1.1) with modifications. Using the continuity relation

$$\frac{m'_b}{\bar{m}_b} = \frac{\rho'}{\bar{\rho}} + \frac{u'_n}{\bar{u}_n} \quad (4.1)$$

and the isentropic relation

$$\frac{\rho'}{\bar{\rho}} = \frac{\bar{\rho}'}{\delta \bar{\rho}} \quad (4.2)$$

equation (1.1) may be rewritten as

$$R_v = \left(\frac{u'_n}{\bar{u}_n} - \frac{\rho'}{\delta \bar{\rho}} (R_p - 1) \right) \frac{u'_t}{\bar{u}} \quad (4.3)$$

The conditions at the propellant surface are not isentropic; however, for lack of an alternative, the above substitution has been used to eliminate the density ratio from the expression for R_v .

All quantities on the right-hand side of equation (4.3), except for the perturbation velocity (u'_n) are known at the propellant surface from either measurements downstream of the propellant or by simple computation (see Appendix 1).

Because of the hostile environment near the burning propellant, the perturbation velocity at the propellant surface cannot easily be measured directly. The perturbation velocity at the propellant surface is, however, a boundary condition to the system of differential equations which governs the flow within the combustion chamber.

In principle, the general solution of the governing equations along with the experimental pressure measurements should allow easy computation of the boundary condition u_{∞}' . The correct boundary condition u_{∞}' would force the general solution for the pressure distribution to match the measured pressure distribution at the points along the length of the Rv-measurement apparatus where the pressure measurements were taken. The velocity-coupled response function (Rv) would then be known from equation (4.3).

Unfortunately, the governing equations do not lend themselves to a closed form solution. In light of this, the following numerical data reduction procedure has been developed.

- Step (1) Assume a value for Rv.
- Step (2) Calculate the boundary condition u_{∞}' using equation (4.3).
- Step (3) Use u_{∞}' along with the remaining boundary conditions to numerically solve for the pressure distribution within the experimental device.
- Step (4) Compare the calculated pressure distribution to

the experimentally measured pressure distribution.

Step (5) Choose a new R_v on the basis of the results of the comparison.

Step (6) Repeat steps (2) through (5) until the measured and computed values agree to within prescribed limits.

Steps (3), (4) and (5) will be discussed in greater detail in the following sections.

Since the velocity-coupled response function is a physical property of solid propellants, it is expected that the iterative procedure presented here will converge to a unique value. The validity of the final result can be checked by comparing the experimentally measured pressure distribution to the pressure distribution that would result from the R_v value found.

5.0 Numerical Solution of the Governing Equations

Step (3) of the data reduction procedure requires the computation of the perturbation pressure p' as a function of the axial distance from the propellant sample. A fourth-order Runge-Kutta numerical technique has been used. The discussion here will show how the governing equations have been reduced to the form required by the RK-4 numerical integration algorithm.

5.1 Governing Equations

The equations which govern the fluid flow within the experimental device are

- (1) conservation of mass
- (2) conservation of momentum
- (3) conservation of energy, and
- (4) ideal equation of state.

Written in differential form these equations are

$$\frac{\partial \rho}{\partial t} + u \frac{\partial \rho}{\partial x} + \rho \frac{\partial u}{\partial x} = 0 \quad (5.1.1)$$

$$\rho \frac{\partial u}{\partial t} + \rho u \frac{\partial u}{\partial x} + \frac{\partial p}{\partial x} = 0 \quad (5.1.2)$$

$$\frac{\partial p}{\partial t} + u \frac{\partial p}{\partial x} - \gamma \rho \frac{\partial u}{\partial x} = 0 \quad (5.1.3)$$

$$p = \rho R T \quad (5.1.4)$$

The energy equation (5.1.3) incorporates the ideal equation of state, and is approximately valid for negligible heat conductivity of the combustion product gases. Furthermore, convective and radiative processes are considered to make negligible contributions to the energy equation.

Since the flow within the combustion chamber involves both mean and perturbation flows, it is convenient to separate the two as follows

$$\begin{aligned}\rho &= \bar{\rho} + \rho' \\ \rho &= \bar{\rho} + \rho' \\ u &= \bar{u} + u' \\ \tau &= \bar{\tau} + \tau'\end{aligned}\quad (5.5.5)$$

Furthermore, the perturbations are periodic so that

$$\begin{aligned}\rho' &= \rho_0 e^{i\omega t} \\ \rho' &= \rho_0 e^{i\omega t} \\ u' &= u_0 e^{i\omega t}\end{aligned}\quad (5.5.6)$$

For periodic functions, the time-derivative operator reduces to $i\omega$, enabling the governing equations to be treated as ordinary differential equations.

Neglecting second-order effects the governing equations reduce to the following when substitutions (5.1.5) and (5.1.6) are made.

Continuity

$$\bar{\rho} \frac{\partial \bar{u}}{\partial x} + \bar{u} \frac{\partial \bar{\rho}}{\partial x} = 0 \quad (5.1.7)$$

$$\bar{\rho} \bar{u} \rho' + u' \frac{\partial \rho'}{\partial x} + \bar{\rho} \frac{\partial u'}{\partial x} + \rho' \frac{\partial \bar{u}}{\partial x} + \bar{u} \frac{\partial \rho'}{\partial x} = 0 \quad (5.1.8)$$

Momentum

$$\bar{\rho} \bar{u} \frac{\partial \bar{u}}{\partial x} + \frac{\partial \bar{\rho}}{\partial x} = 0 \quad (5.1.9)$$

$$\rho' \bar{u} \bar{u} u' + \bar{\rho} \bar{u} \frac{\partial u'}{\partial x} + \bar{\rho} u' \frac{\partial \bar{u}}{\partial x} + \rho' \bar{u} \frac{\partial \bar{u}}{\partial x} + \frac{\partial \bar{\rho}'}{\partial x} = 0 \quad (5.1.10)$$

Energy

$$\bar{\rho} \bar{u} C_v \frac{\partial \bar{T}}{\partial x} + \bar{\rho} \frac{\partial \bar{u}}{\partial x} = 0 \quad (5.1.11)$$

$$\bar{\rho} C_v u T' + \bar{\rho} \bar{u} C_v \frac{\partial T'}{\partial x} + \bar{\rho} u' C_v \frac{\partial \bar{T}}{\partial x} + \rho' \bar{u} C_v \frac{\partial \bar{T}}{\partial x} + \rho' \frac{\partial \bar{u}}{\partial x} + \bar{\rho} \frac{\partial \bar{u}'}{\partial x} = 0 \quad (5.1.12)$$

Equation of State

$$\bar{\rho} = \bar{\rho} R \bar{T} \quad (5.1.13)$$

$$\rho' = \bar{\rho} R T' + \rho' R \bar{T} \quad (5.1.14)$$

Assuming that the mean flow Mach number of the flow normal to the propellant is much less than 1, terms

containing \bar{u}^2 can be neglected. Rearrangement of the previous equations under the assumption of negligible mean flow Mach number yields the following equations.

$$\frac{\partial \bar{F}}{\partial x} = 0 \quad (5.1.15)$$

$$\frac{\partial \bar{p}}{\partial x} = -\frac{\bar{\rho}}{\bar{F}} \frac{\partial \bar{F}}{\partial x} \quad (5.1.16)$$

$$\frac{\partial \bar{u}}{\partial x} = \frac{\bar{q}}{\bar{F}} \frac{\partial \bar{F}}{\partial x} \quad (5.1.17)$$

$$\frac{\partial \bar{u}'}{\partial x} = -\frac{1}{\bar{\rho} \bar{p}} \frac{\partial \bar{p}}{\partial x} - \frac{\bar{u}}{\bar{\rho} \bar{p}} \frac{\partial \bar{p}}{\partial x} \bar{u}' + \frac{1}{\bar{\rho} \bar{p}} (\bar{\rho} \bar{u}' \bar{u} - \bar{\sigma} \bar{p}') \frac{\partial \bar{u}}{\partial x} \quad (5.1.18)$$

$$\frac{\partial \bar{\rho}'}{\partial x} = -\bar{\rho} \bar{u}' \bar{u}' - \bar{\rho} \bar{u} \frac{\partial \bar{u}'}{\partial x} - \bar{\rho} \bar{u}' \frac{\partial \bar{u}}{\partial x} \quad (5.1.19)$$

These equations are in the form required by the Runge-Kutta numerical algorithm for integration. If the temperature distribution $T(x)$ is known, these equations along with the boundary conditions at the propellant surface, are sufficient to calculate the pressure distribution (p') along the length of the experimental device.

5.2 Boundary Conditions

The boundary conditions required at the propellant surface are listed below

- mean pressure
- mean density
- mean velocity
- perturbation pressure
- perturbation velocity

For the purpose of this investigation, typical values for the above quantities will be used. The values used, along with other environmental parameters are given in Appendix 1.

5.3 Temperature Distribution

Since the heat flux through the measurement apparatus wall is unknown the mean flow temperature distribution $T(x)$ cannot be found directly. However, the following approximate expression for the temperature distribution using the one-dimensional steady-state heat diffusion equation has been used.

$$T(x) = (T_0 - T_\infty) e^{-\lambda x} + T_\infty \quad (5.3.1)$$

where

$$\lambda = 2 \frac{k_2}{k_1} \frac{1}{r \sigma t}$$

and, k_2 and k_1 are the thermal conductivities of the combustion gas and the apparatus wall respectively.

In the future, it may be necessary to refine the above temperature distribution to incorporate three-dimensional effects.

6.0 Error Function

In order to compare the numerical solution for the pressure distribution to the measured pressure distribution, the following least-squares error function has been considered

$$E(R_v) = \sum_{i=1}^N (p_{m,i}' - p_{n,i}')^2 \quad (6.1)$$

where N is the number of pressure measurements taken at selected points along the length of the experimental Rv-measurement device. The quantities p_m' and p_n' are the measured and calculated pressures at the i'th selected pressure port.

The quantities R_v , p_m' and p_n' in equation (6.1) are complex. The velocity-coupled response function is complex since the velocity-coupled response is not generally in phase with the tangential velocity perturbations. Also, the perturbation pressure is complex having both magnitude and phase. Consequently, the error function E is a complex function. It is meaningless, therefore, to consider minimizing E as defined by equation (6.1). In light of this, the following approaches have been considered.

- (1) Minimize both the real and imaginary components of E simultaneously.
- (2) Minimize the magnitude of E only.
- (3) Minimize the phase angle of E only.

All three approaches are valid since both the magnitude

and phase of the perturbation pressure distribution are unique for a given velocity coupled response function (R_v). As will be shown in Appendix 5, the use of the phase distribution provides the smoothest error function (E), and consequently, equation (6.1) has been modified through the use of the phase angles of the perturbation pressures. Thus the error function, $E(R_v)$, given by

$$E(R_v) = \sum_{i=1}^N (\langle p_m'_i \rangle - \langle p_n'_i \rangle) \quad (6.2)$$

is a real valued function of two independent variables. The symbol $\langle \cdot \rangle$ denotes the angular component of the perturbation pressure. The independent variables are the real and imaginary components of R_v .

The desired value of R_v is that which minimizes the above error-function. When E is minimized, the pressure distribution which has been calculated by numerically integrating the governing equations will match the measured pressure distribution as closely as possible at the N selected points.

7.0 Location of Pressure Ports

As mentioned in the previous section, the numerical solution for the perturbation pressure distribution can be fitted to the measured distribution at selected points along the length of the experimental device. The experimental apparatus has provisions for measurement of pressure at numerous locations along its length. The positions of the pressure measurement will affect the performance of the curve-fit procedure. The optimum location of these pressure measurements is at the part of the curve where variation is greatest since the shape of the curve will be most sensitive to slight variations in admittance value. Perturbation pressure phase distributions are provided in Appendix 5 for a wide range of admittance values and a driver frequency of 600 hertz. From these figures it can be seen that maximum variation of the curves occurs in the region between 0.100 meters and about 0.150 meters along the length of the Rv-measurement apparatus. The locations of the pressure measurements have been chosen to be at ten equally spaced locations from 0.100 meters to 0.145 meters along the length of the apparatus.

8.0 Optimization Procedure

8.1 BFGS Optimization Algorithm

The BFGS (Broyden, Fletcher, Goldfarb, Shanno) numerical optimization algorithm (Ref.4) has been used to minimize the error function (equation 6.2). Since the velocity-coupled response function (Rv) is complex, the domain has been considered to be the R^2 plane with the X_1 -coordinate representing the real part of Rv and the X_2 -coordinate representing the imaginary part of Rv .

Most search algorithms involve a line search given by the following equation

$$x_{k+1} = x_k - \alpha H_k \nabla y(x_k) \quad (8.1.1)$$

where y is the function of interest. For a gradient search, H_k is the unit matrix (I) and α is the parameter of the gradient line. for Newton's method H_k is the inverse of the Hessian matrix, H_k^{-1} , and α is 1. The Hessian (H_k) is the matrix of second partial derivatives evaluated at the point x_k . For quasi-Newton methods, H_k is a series of matrices beginning with the identity matrix, I , and ending with the inverse of the Hessian matrix (H_k^{-1}). The quasi-Newton algorithm that employs the BFGS formula for updating the Hessian matrix is considered to be the most effective of the unconstrained multivariable search techniques, according to Fletcher (Ref. 5).

The minus sign in equation (7.1) indicates the

direction of steepest descent and a positive sign in the equation would give the direction of steepest ascent. However, equation (7.1) is really steep descent rather than steepest descent. Only if the function of interest, the error function, is scaled such that a unit change in each of the independent variables reduces the same unit change in the error function will the gradient move in the direction of steepest descent. Scaling is a problem that has been encountered during this investigation. It was resolved by multiplying the real and imaginary components of the admittance by 1000.

The BFGS algorithm is outlined in what follows.

- (1) Choose starting point $Rv - x_{k+1}$.
- (2) Compute gradient $E(x_k)$ using a forward difference approximation.
- (3) Form the Hessian matrix given below.

$$H_{k+1} = H_k + \left[\frac{H_k \gamma_k \delta_k^T + \delta_k \gamma_k^T H_k}{\delta_k^T \gamma_k} \right] + \left[\frac{\gamma_k^T H_k \gamma_k}{\delta_k^T \gamma_k} \right] \left[\frac{\delta_k \delta_k^T}{\delta_k^T \gamma_k} \right] \quad (8.1.2)$$

where $\delta_k = x_{k+1} - x_k$ and $\gamma_k = \nabla E(x_{k+1}) - \nabla E(x_k)$

- (4) Form the gradient line given below.

$$x_{k+1} = x_k - \alpha_{k+1} H_k \nabla E(x_k) \quad (8.1.3)$$

- (5) Search for parameter α_{k+1} , which minimizes the error function (E) along the gradient line. This is described in detail in the next section.
- (6) Compute x_{k+1} .
- (7) Repeat steps (2) through (6) until convergence.

As mentioned previously, the initial value for the Hessian matrix is the identity matrix.

The algorithm generates a sequence of values x_k that move rapidly from the starting point x_0 to the neighborhood of the optimum x^* and terminate when the difference between successive iterations is less than some prescribed value.

The value of the parameter α which minimizes the error function along the gradient line is found by a Fibonacci line search. The Fibonacci line search algorithm is discussed in the following in the following section.

8.2 Fibonacci Line Search

To find the optimum of a search problem, a search plan is required. A search plan is a set of instructions for performing N sets of "experiments" x_1, x_2, \dots, x_N (values of the independent variables). In this discussion, an "experiment" will consist of specifying the value of the independent variable (α) and determining the value of the function $E(\alpha)$ for that specified value.

The Fibonacci search (Ref. 4) will be used to search for the parameter α which minimizes the error function (E) along the gradient line (equation 8.1.1). Values for range from 0 to 1 generating points along the line from x_0 to x_{k+1} .

The first step of the Fibonacci search requires the calculation of the number of experiments required to reduce the final interval of uncertainty in α to within tolerable limits. This desired final interval of uncertainty

(I_n) is given by the following equation.

$$I_n = \frac{I_0}{A_{n+1}} \quad (8.2.1)$$

where I_0 is the initial interval, and A_{n+1} is the $(n+1)^{\text{th}}$ Fibonacci number. The initial interval (I_0) is 1 since the parameter α has possible values ranging from 0 to 1.

The Fibonacci numbers are generated as follows

$$A_1 = 1$$

$$A_2 = 2$$

$$A_i = A_{i-1} + A_{i-2} \quad \text{for } i > 2$$

The number of experiments required to reduce the interval of uncertainty from $I_0 = 1$ to I_n is the smallest value n such that

$$A_{n+1} \geq \frac{I_0}{I_n} \quad (8.2.3)$$

The values of α for the first two experiments are the following

$$\alpha_1 = A_{n-1}, I_n = A_{n-1} \left\{ \frac{I_0}{A_{n+1}} \right\} \quad (8.2.4)$$

$$\alpha_2 = A_n, I_n = A_n \left\{ \frac{I_0}{A_{n+1}} \right\} \quad (8.2.5)$$

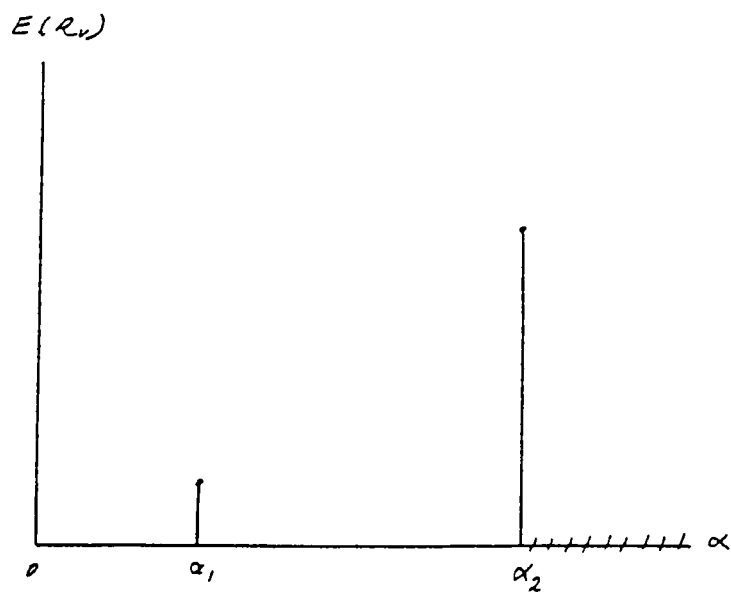
The position of α_1 is symmetrically to α_2 , a distance I_2 from the upper bound of the interval.

The procedure continues after the first two experiments are evaluated by discarding the interval that does not contain the minimum. It is important to realize that the

function is assumed to be unimodal along the gradient line. The error function (equation 6.2) is not unimodal. However, it has been found that the distances between local minimums is large with respect to typical gradient line lengths.

The third experiment is placed in the remaining interval symmetrically to the one which was not in the discarded interval. The procedure is continued by placing the remaining experiments symmetrically to the previous one with the best value until the final experiment is placed.

The procedure is best illustrated by the following figures.

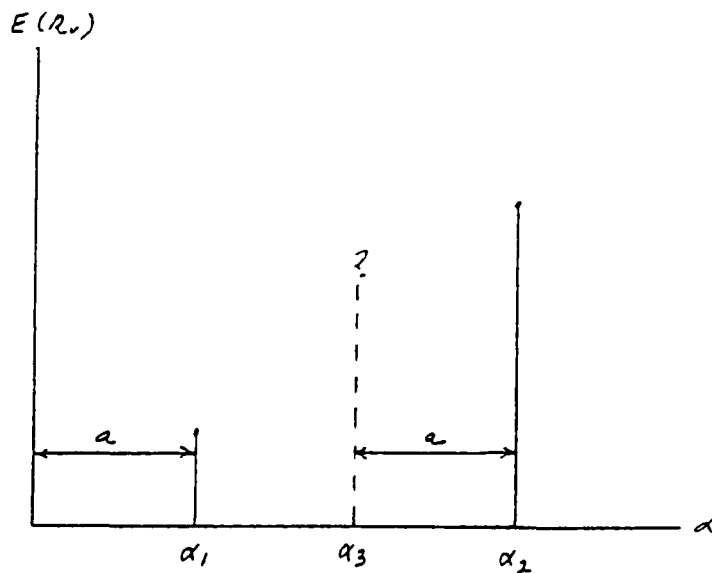


Error Function along Gradient Line

Figure 8.2.1

Suppose $E(\alpha_2) > E(\alpha_1)$ then by unimodality the interval $[\alpha_1, 1]$ would not contain the minimum. Therefore, it is discarded and the second interval of uncertainty is then $[0, \alpha_2]$.

The third experiment is placed symmetrically to α_1 in the remaining interval as illustrated below.



Error Function along Gradient Line

Figure 8.2.2

The remaining experiments are placed in a similar manner until the desired final interval of uncertainty I_n is obtained. The optimal value for α is then taken to be either the upper bound or the lower bound the final interval of uncertainty depending on whether the previously discarded

interval was to the right or left. Since the final interval is chosen to be small, any point in that interval could be used as the optimal value.

9.0 Description of Computer Program

The data reduction program consists of a Runge-Kutta routine driven by a BFGS multivariable search routine. The Runge-Kutta solves the governing equation for the perturbation pressure distribution within the experimental device for a specified admittance value of the solid propellant. The following sections will discuss the admittance to velocity-coupled response function conversion, the Runge-Kutta algorithm and the BFGS multivariable search algorithm in greater detail.

9.1 Admittance to Velocity-Coupled Response Function Conversion

The admittance (Y) of a solid propellant is defined by the following equation.

$$\frac{\partial \bar{u}_n'}{\partial x} = Y \frac{\partial \bar{p}'}{\partial p} \quad (9.1.1)$$

An expression for the perturbation velocity is obtained by rearranging equation (4.3).

$$\bar{u}_n' = \bar{u}_n \frac{\partial \bar{p}'}{\partial p} (R_p - 1) + R_v \bar{u}_n \frac{\bar{u}_e'}{\alpha} \quad (9.1.2)$$

Upon elimination of the normal perturbation velocity from the above equations the following relationship between the admittance and the velocity-coupled response function is obtained.

$$Y = \frac{\partial \bar{u}_n}{\alpha} (R_p - 1) + \frac{\partial \bar{u}_n}{\bar{g}_n} \frac{\bar{p}}{p'} \bar{u}_e' R_v \quad (9.1.3)$$

Program 2 (Appendix 3) has been written to perform the above conversion.

9.2 Runge-Kutta Algorithm

A fourth-order Runge-Kutta algorithm (Ref. 6) is used to determine the perturbation pressure distribution by integration of the governing equations (5.1.15) through (5.1.19). The input to the algorithm consists of the environmental parameters and the boundary conditions at the propellant surface. Typical values for the environmental parameters and all boundary conditions except for the perturbation velocity (u_{∞}') at the propellant surface are given in (Appendix 1). For calculation of the velocity-coupled response function for a particular propellant sample in a specified environment all input quantities except for u_{∞}' are fixed. This boundary condition is determined by admittance values which are generated according to the multivariable search procedure. For a particular admittance value, the perturbation velocity (u_{∞}') is given by

$$u_{\infty}' = \gamma \bar{q} \frac{\partial' p}{\partial \bar{p}} \quad (9.2,1)$$

The step size (H) governs the locations at which the perturbation pressures are calculated. It is important that the perturbation pressure be calculated at points along the length of the experimental device where pressure measurements are made. Improved accuracy can be obtained by decreasing the step size (H). Alternatively, the step size can be adjusted in the middle of the calculation to accommodate a pressure distribution that is rapidly varying.

9.3 BFGS Optimization Algorithm

The purpose of this algorithm is to search for the particular admittance value which provides the boundary condition (u'_∞) which, when used as input to the Runge-Kutta routine, yields the pressure distribution matching the measured pressure distribution.

The BFGS algorithm has been encoded into a main program, two subroutines and three function subroutines.

The three function subroutines are as follows. The function FUNCT contains the function to be minimized (equation 6.2). The function F uses FUNCT for the value of the error function in the line search. The function FIBON uses the values of F in the Fibonacci line search. The two subroutines are slope, which evaluates the partial derivatives using a forward difference approximation, and PRINT, which prints the results of the computations.

The input variables for the BFGS routine are the starting point (\mathbf{Y}_0) and the stopping criterion. The program will terminate when the difference between the error function values of two successive iterations is less than or equal to the stopping criterion. The output results are the iteration number, the value of the error function, and the admittance value.

The main portion of the BFGS algorithm proceeds from iteration zero, the starting point, and generates successive points until the stopping criterion is met. Initially, the Hessian matrix (\mathbf{H}) is the identity matrix. The gradient is

computed using a forward difference approximation of the partial derivatives (using subroutine SLOPE). The Fibonacci search function, FIBON, is used to locate the minimum along the gradient line from x_A to x_{A+1} . Then the stopping criterion is checked, and the Hessian matrix is stored in ERROLD for future comparisons. The search direction to the next point is calculated and stored in the vector S. The value of the parameter of the line in the search direction, K, is calculated using FIBON to locate the next point. The value of the error function at the new point is calculated and stored in ERR. The values of the iteration counter, the function at the new point, and the new point are printed using PRINT. The values of the gradient at the current point are computed and stored in the vector GRAD. The Hessian matrix is updated, and the program returns to repeat the calculation until the error criterion is satisfied.

10.0 Simulation of Experiment

For the purpose of testing the data reduction program, experimental pressure phase angle data have been simulated by introducing random fluctuations in calculated pressure phase angles for specific values of admittance. Experimental data was simulated for two admittance values: (0.04,-0.02) and (0.00,0.02). Program 3 (Appendix 4) was used to obtain random fluctuations from gaussian distributions having standard deviations ranging from zero through five degrees.

Using the simulated data, the program was tested to see whether or not convergence to the above admittance values from an arbitrary starting point was attained. The results are presented in the following section.

11.0 Simulation Results

Results are presented here for two sample runs of the data reduction program. Using admittance values of (0.04,-0.02) and (0.00,0.,02) the perturbation pressure distribution was calculated. The following computer printouts show the results for random fluctuations in input pressure data ranging from zero to five degrees. The performance of the data reduction program has proven to be satisfactory for perturbation pressure phase measurement data having random fluctuations of less than five degrees.

The velocity-coupled response function values corresponding to the admittance values were found using Program 2 (Appendix 3) to be (0.15,0.48) and (-0.19,0.13) for the respective admittance values (0.04,-0.02) and (0.00,0.02). It was necessary to assume a value for the pressure-coupled response function to perform the above conversion. The value used for R_p was (0.1,-0.1). Since the pressure-coupled response of solid propellants was not investigated, the admittance to R_v conversion was not included in the main data reduction program.

The test results are summarized at the end of this section. The summary table shows the admittance values which were recovered when pressure phase data corresponding to the above two admittance values were input. It is clear from these results that performance of the data reduction program is generally good when random fluctuations in the input pressure phase data does not exceed four degrees.

Standard Deviation in Random Error of Input Data = 0 degrees

EFIDI-FIEONACCI SEARCH FOR ADMITTANCE

INPUT DATA:

Stopping Criterion .5000

Starting Point (Y₀) 5.00 10.00

Experimental Pressure Phase Values (degrees)

F(1) = 93.962
F(2) = 95.161
F(3) = 97.294
F(4) = 102.203
F(5) = 114.158
F(6) = -120.802
F(7) = -101.871
F(8) = -97.054
F(9) = -95.016
F(10) = -93.856

RESULTS:

Iteration	Error Function	Y X 1000	
0	145.157	5.000	10.000
1	2.705	-1.521	10.521
2	.265	14.1	10.565
3	.155	.142	10.565

NORMAL TERMINATION OF PROGRAM

Standard Deviation in Random Error of Input Data = 1 degree

EFGS-FIECI-ACCI SEARCH FOR ADMITTANCE

INPUT DATA:

Stopping Criterion 5000

Starting Point (Y₀) 5.00 10.00

Experimental Pressure Phase Values (degrees)

F(1) = 64.364
P(2) = 55.040
F(3) = 58.703
F(4) = 101.274
F(5) = 124.553
F(6) = -121.193
F(7) = -100.645
F(8) = -94.231
F(9) = -55.486
F(10) = -63.295

RESULT:

Iteration	Error Function	Y X 1000	
0	144.550	5.000	10.000
1	14.556	116	18.661
2	13.059	291	13.176
3	13.059	.291	13.176

NORMAL TERMINATION OF PROGRAM

Standard Deviation in Random Error of Input Data = 2 degrees

EFAS-FIECHACCI SEARCH FOR ADMITTANCE

INPUT DATA:

Stopping Criterion 5000

Starting Point (x,y) 10.00 15.00

Experimental Pressure Phase Values (degrees)

$E(1) = 67.113$
 $E(2) = 67.797$
 $E(3) = 65.975$
 $E(4) = 64.569$
 $E(5) = 63.552$
 $E(6) = 62.619$
 $E(7) = 61.866$
 $E(8) = 60.951$
 $E(9) = 60.166$
 $E(10) = 59.401$

RESULTS:

Iteration	Search Function	$\times 10^3$	$\times 10^3$
0	67.113	0.000	15.000
1	67.797	-0.000	14.995
2	65.975	-0.000	14.985
3	64.569	-0.000	14.976

SEARCH TERMINATION OF FIECHACCI

Standard Deviation in Random Error of Input Data = 3 degrees

EFCS-FIECMACCI SEARCH FOR ADMITTANCE

INPUT DATA:

Stopping Criterion 5000

Starting Point (Y₀) 10.00 15.00

Experimental Pressure Phase Values (degrees)

P(1) = -60.158
P(2) = -62.678
P(3) = 100.565
P(4) = 101.065
P(5) = 121.445
P(6) = -120.605
P(7) = -95.135
P(8) = -95.560
P(9) = -95.055
P(10) = -97.027

RESULTS:

Iteration	Error Function	Y x 1000	
0	520.142	10.000	15.000
1	56.426	.645	12.441
2	26.600	.170	16.029
3	18.591	-.182	16.131

NORMAL TERMINATION OF PROGRAM

Standard Deviation in Random Error of Input Data = 4 degrees

EFGE-FIECMACCI SEARCH FOR ADMITTANCE

INPUT DATA:

Stopping Criterion 0100

Starting Point (Y) 5.00 10.00

Experimental Pressure Phase Values (degrees)

F(1) = 59.064
F(2) = 98.413
F(3) = 64.666
F(4) = 101.513
F(5) = 121.667
F(6) = -116.263
F(7) = -99.870
F(8) = -92.926
F(9) = -93.959
F(10) = -97.452

RESULTS:

Iteration	Error Function	Y X 1000	
0	116.565	5.000	10.000
1	67.970	5.110	17.323
2	54.350	5.211	17.424
3	54.350	5.211	17.424

NORMAL TERMINATION OF FREGFPM

Standard Deviation in Random Error of Input Data = 5 degrees

EFGS-FIEOMACCI SEARCH FOR ADMITTANCE

INPUT DATA:

Stopping Criterion .0100

Starting Point (Y₀) 5.00 15.00

Experimental Pressure Phase Values (degrees)

F(1) = -50.007
F(2) = 94.544
F(3) = 96.881
F(4) = 101.513
F(5) = 114.159
F(6) = -128.118
F(7) = -103.380
F(8) = -95.704
F(9) = -101.160
F(10) = -85.622

RESULTS:

Iteration	Error Function	Y X 1000	
0	450.169	5.000	15.000
1	424.472	2.424	15.000
2	189.223	-1.143	26.756
3	186.226	-1.143	26.756

NORMAL TERMINATION OF PROGRAM

Standard Deviation in Random Error of Input Data = 0 degrees

EFGS-FIELMACCI SEARCH FOR ADMITTANCE

INPUT DATA:

Stopping Criterion .5000

Starting Point (Y₀) 30.00 -25.00

Experimental Pressure Phase Values (degrees)

F(1) =	86.505
F(2) =	85.244
F(3) =	82.700
F(4) =	74.61E
F(5) =	-21.187
F(6) =	-77.341
F(7) =	-83.329
F(8) =	-85.50E
F(9) =	-88.637
F(10) =	-87.335

RESULTS:

Iteration	Error Function	Y X 1000'
0	1506.887	30.000 -25.000
1	.237	40.350 -20.175
2	.179	40.306 -20.079

NORMAL TERMINATION OF PROGRAM

Standard Deviation in Random Error of Input Data = 1 degree

EFGE-FIECMACCI SEARCH FOR ADMITTANCE

INPUT DATA:

Stopping Criterion .5000

Starting Point (Y₀) 30.00 -25.00

Experimental Pressure Phase Values (degrees)

F(1) = 86.507
F(2) = 85.123
F(3) = 84.109
F(4) = 73.887
F(5) = -20.487
F(6) = -77.632
F(7) = -82.303
F(8) = -82.673
F(9) = -87.110
F(10) = -86.777

RESULTS:

Iteration	Error Function	Y x 1000
0	1592.050	30.000 -25.000
1	12.12E	40.680 -20.0E2
2	12.057	40.629 -19.991

NORMAL TERMINATION OF PROGRAM

Standard Deviation in Random Error of Input Data = 2 degrees

EFGE-FIECMACCI GEAPCF FCR ADMITTANCE

INPUT DATA:

Stopping Criterion 5000

Starting Point (Y₀) 10.00 -25.00

Experimental Pressure Phase Values (degrees)

F(1) =	16.561
F(2) =	87.680
F(3) =	21.391
F(4) =	77.414
F(5) =	-25.883
F(6) =	-77.757
F(7) =	-93.524
F(8) =	-64.513
F(9) =	-25.417
F(10) =	-85.313

RESULTS:

Iteration	Error Function	Y X 1000
0	1183.286	10.000 -25.000
1	25.490	18.570 -21.032
2	25.302	18.570 -20.647

NORMAL TERMINATION OF PROGRAM

Standard Deviation in Random Error of Input Data = 3 degrees

EFCS-FIECHACCI SEARCH FOR ADMITTANCE

INPUT DATA:

Stopping Criterion .5000

Starting Point (Y₀) 30.00 -25.00

Experimental Pressure Phase Values (degrees)

F(1) = 23.309
F(2) = 82.959
F(3) = 56.571
F(4) = 74.678
F(5) = -16.900
F(6) = -77.346
F(7) = -77.797
F(8) = -82.011
F(9) = -85.574
F(10) = -90.509

RESULTS:

Iteration	Error Function	Y × 1000
0	1973.404	30.000 -25.000
1	79.720	42.246 -19.447
2	79.721	42.249 -19.447

NORMAL TERMINATION OF PROGRAM

Standard Deviation in Random Error of Input Data = 4 degrees

EFGE-FIECHACCI SEARCH FOR ADMITTANCE

INPUT DATA:

Stopping Criterion .5000

Starting Point (Y0) 30.00 -25.00

Experimental Pressure Phase Values (degrees)

F(1) =	82.550
F(2) =	84.827
F(3) =	82.297
F(4) =	73.262
F(5) =	-11.186
F(6) =	-84.557
F(7) =	-95.038
F(8) =	-34.146
F(9) =	-52.781
F(10) =	-79.104

RESULT:

Iteration	Error Function	Y X 1000
0	691.610	30.000 -25.000
1	173.712	37.375 -21.803
2	170.172	37.551 -22.737
3	170.172	37.551 -22.737

NORMAL TERMINATION OF PROGRAM

Standard Deviation in Random Error of Input Data = 5 degrees

EFCS-FIBONACCI SEARCH FOR ADMITTANCE

INPUT DATA:

Stopping Criterion .5000

Starting Point (Y₀) 30.00 -25.00

Experimental Frequency Phase Values (degrees)

F(1) =	60.607
F(2) =	86.496
F(3) =	80.372
F(4) =	74.126
F(5) =	-21.655
F(6) =	-72.702
F(7) =	-81.528
F(8) =	-81.428
F(9) =	-85.580
F(10) =	-60.934

RESULT:

Iteration	Error Function	Y × 1000
0	1655.679	30.000 -25.000
1	15.488	41.025 -20.053
2	21.326	41.301 -20.680
3	21.326	41.301 -20.680

NORMAL TERMINATION OF PROGRAM

SUMMARY OF TEST RESULTS

Simulated Input Data for an Admittance Value of (0.00,20).

Standard Deviation of Random Error	Value of Error Function	Starting Point	Value Recovered
0	0.253	(5,10)	(.143,19.6)
1	13.1	(5,10)	(.201,19.2)
2	44.0	(10,15)	(2.05,22.7)
3	88.6	(10,15)	(-.182,16.1)
4	64.4	(5,10)	(2.21,17.4)
5	138	(5,15)	(-.143,29.8)

Simulated Input Data for an Admittance Value of (40,-20).

Standard Deviation of Random Error	Value of Error Function	Starting Point	Value Attained
0	0.179	(30,-25)	(40.3,-20.1)
1	12.1	(30,-25)	(40.6,-20.0)
2	29.3	(30,-25)	(38.6,-20.8)
3	79.7	(30,-25)	(42.2,-19.4)
4	81.3	(30,-25)	(41.3,-20.7)
5	170	(30,-25)	(37.6,-22.7)

(note: all admittance values are multiplied by 1000)

12.0 Conclusion

A data reduction program has been written for the calculation of the velocity-coupled response function of solid propellants from experimentally measured pressure data. The program has been written for use with a new velocity-coupled response function measurement apparatus that is currently being developed at Embry-Riddle Aeronautical University. The data reduction procedure has proven satisfactory for simulated experimental data which have random fluctuations with standard deviations up to four degrees.

13.0 Recommendations for Future Work

The following recommendations for future investigation which are outlined here are based on the possible need for improvements in the performance and accuracy of the data reduction program.

(1) Study the heat transfer between the combustion gases and the surroundings. Revise the approximation for the temperature distribution given by equation (5.3.1).

(2) Investigate the shape of the error function (equation 6.2). Proper scaling of this function will improve the performance of the BFGS optimization routine. The method of steepest descent works best when shape of the error function is parabolic. Procedures for scaling are described in detail by Wilde (Ref. 6) and Wilde and Beightler (Ref. 7).

(3) Investigate other types of error functions for the possibility of obtaining one which is unimodal for the domain of realistic R_v values. For unimodal error functions, the global convergence property assures convergence to the correct solution from any starting point.

References

1. Culick F.E.C., "Stability of Longitudinal Oscillations with Pressure and Velocity Coupling in a Solid Propellant Rocket," Combustion Science and Technology, Vol.2, 1970.
2. Brown R.S., Culick F.E.C. and Zinn B.T., "Experimental Methods for Combustion Admittance Measurements," AIAA Progress in Astronautics and Aeronautics: Solid Propellant Rocket Research, Vol. 1, edited by M. Summerfield, Academic Press, New York, 1960, p.p. 295-358.
3. Brown R.S. and Waugh R.C., "Pressure and Velocity Response Function Measurements by the Rotating Valve Method," Technical Report, United Technologies Corporation, Sunnyvale, Calif., 1978.
4. Pike R.W., Optimization for Engineering Systems, Van Nostrand Reinhold Company, New York , 1986.
5. Fletcher, R., Practical Methods of Optimization, John Wiley and Sons, Inc., New York, 1981.
6. Johnston R.L., Numerical Methods: A Software Approach, John Wiley and Sons, Inc., Toronto, 1982.
7. Wilde, D.J., Optimum Seeking Methods, Prentice-Hall, Inc., Englewood Cliffs, N.J., 1964.

8. Wilde, D.J., and Beightler C.S., Foundations of Optimization, Prentice-Hall, Inc., Englewood Cliffs, N.J., 1967.

Appendix 1: Input Data

Typical values for environmental parameters are given below. The variable names used are the same as those used in the computer program.

ratio of specific heats: GAM - 1.4

universal gas constant: R .. 287 J/kgK

specific heat at constant volume: CV = 717 J/kgK

conductivity of combustion gases: K1 30 W/mK

conductivity of apparatus wall: K2 - 40 000 W/mK

radius of apparatus: RADIUS 0.05 m

length of apparatus: LENGTH 0.01 m

ambient temperature: TINF 273 K

The following are boundary conditions for the variables at the propellant surface.

mean pressure: P0 = 101320 Pa

perturbation pressure: PPO = (0,1200) Pa

density: RH00 - 1.226 kg/m³

temperature: TNOT = 3500 K

The mean flow velocity (\bar{u}_λ) at the propellant surface can be calculated from continuity and the propellant mass burn rate. The mass flow (\dot{m}) is related to the mass burn rate by

$$\dot{m} = r_b \rho_b A_b \quad (A.1)$$

The continuity relation is

$$\dot{m} = \bar{u}_n \bar{\rho} A_b \quad (A.2)$$

Equating (A.1) and (A.2), the following expression for the mean flow velocity is obtained

$$\bar{u}_n = \frac{r_b \rho_b}{\bar{\rho}} \quad (A.3)$$

Typical values for the quantities in equation (A.3) are given below

mass burn rate: $r_b = 0.0063 \text{ kg/s}$

propellant density: $\rho_b = 1200 \text{ kg/m}^3$

exhaust gas density: $\bar{\rho} = 1.226 \text{ kg/m}^3$

The mean flow normal velocity at the propellant surface is then

mean flow velocity: $u_0 = 6 \text{ m/s}$

The frequency of the standing acoustic wave was given a value of 600 hertz. This value is within the frequency range at which the Rv-measurement apparatus is expected to be operated. The angular frequency is then $2 \times 3.14 \times 600 \text{ Hz}$.

angular frequency of acoustic wave: $\omega = 3770 \text{ rad/s}$

It is necessary that the mass flow perturbation frequency be identical to the acoustic frequency. This requirement is met if the propellant sample is oscillated at one-half the acoustic frequency since the mass flow response is not sensitive to the direction of the tangential perturbation velocity.

The average tangential velocity obtained by integrating over one period is

$$\overline{u_t'} = \frac{2}{\pi} \overline{u'_o} \quad (1.4)$$

where $\overline{u'_o}$ is the maximum value obtained by the tangential perturbation velocity. A typical value for $\overline{u'_o}$ is 30 m/s. The mean tangential perturbation velocity from the previous equation is 19 m/s.

Appendix 2: Data Reduction Program

This appendix contains a listing of the data reduction program. This program determines the admittance value of the propellant. The admittance to velocity-coupled response function conversion is performed by Program 2 (Appendix 3).

Program 1

```

11  CONTINUE
110 FORMAT( '          P(1,12,:) =',F8.3)
      WRITE(1,601)
601 FORMAT( /,/, 'RESULTS ',  

     &      /,/, 'Iteration',10X,'Error Function',10X,'Y X 1000 ',/)

C
C   BFGS SEARCH
C

      ERR= FUNCT(  )
      CALL PRINT( ITER, NTEFM, EFP, X, F )
      CALL SLOPE( GRAD, ERR )

C
C   FORM THE IDENTITY MATRIX
C

      DO 40 I=1,NTERM
        DO 40 J=1,NTERM
          IF (I .NE. J) HESS(I,J)= 0.0
          IF (I .EQ. J) HESS(I,I)= 1.0
40    CONTINUE
50    CONTINUE

      ERROLD= ERR
      ITEM= 1TEFM + 1

C
C   S(I) ~ HESSIAN * GRADIENT
C

      DO 50 I=1,NTERM
        S(I)= 0.0
        DO 50 J=1,NTERM
          S(I)= S(I) + HESS(I,J) * GRAD(J)
50    CONTINUE

C
C   k = ALPHAS IN SECTION 9.3
C

      K= FIPON( DUMMY )

C
C   DETERMINE NEXT X
C

      DELTA= ALPHAS * HESSIAN * GRADIENT

C
C   DO 60 I=1,ITER
        TELTA(I)= K * S(I)
        X(I)= X(T) + TELTA(I)
60    CONTINUE
      EFP= FUNCT( X )
      CALL SLOPE( GRAD, EFP )

C
C   DETERMINE NEW BFGS MATRIX
C

      DPG= 0.0
      DO 70 I=1,NTERM
        GAMMA(I)= GRAD(I) - GRAD(I)
        DPG= DPG + GAMMA(I) * DELTA(I)

```

```

70  CONTINUE
    DO 80 I=1,NTERM
        GRAD(I)= GRADI(I)
80  CONTINUE
    GPHG= 0.0
    DO 90 I=1,NTERM
        HG(I)= 0.0
        DO 90 J=1,NTERM
            HG(J)= HG(I) + HESS(I,J) * GAMMA(J)
            GPHG= GPHG+ HESS(I,J) * GAMMA(I) * GAMMA(J)
90  CONTINUE
    DO 100 I=1,NTERM
        DO 100 J=1,NTERM
            HESS(I,J)= HESS(I,J) - (HG(I) * DELTA(J) / DPG)
3              - (DELTA(J) * HG(J) / DPG)
4              + (1 + (GPHG / DPG)) * DELTA(J)
5              * DELTA(J) / DPG
100 CONTINUE
    TOLER = DABS(ERR-ERR0)
    IF (TOLER .GE. EPS) CALL PRINT(1,ITER,NTERM,ERR,1,K)
    IF (TOLER .GE. EPS) GO TO 20
    CALL PRINT(ITER,NTERM,ERR,X,K)
    WRITE(1,*)
    WRITE(1,*) ' NORMAL TERMINATION OF PROGRAM'
    STOP
END

```

```

C
C      COMPUTATION OF PARTIAL DERIVATIVES
C

```

```

SUBROUTINE SLOPE( DERIV, E )
DOUBLE PRECISION DERIV(I), E, DELTA, TEMPX, Y, X(1), B(6), FUNCT
COMMON X, S, NTERM
DO 30 I=1,NTERM
    DELTA= 1.0E-04
    TEMPX= X(I)
    X(I)= X(I) + DELTA
    Y= FUNCT( X )
    DERIV(I)= (Y - E)/DELTA
    X(I)= TEMPX
30  CONTINUE
RETURN
END

```

```

C
C      PRINT RESULTS
C

```

```

SUBROUTINE PRINT( I, N, VAL, ' ' )
DOUBLE PRECISION X(20),VAL,R
WRITE(1,*) I,VAL,(Y(J),J=1,N)
501 FORMAT(1X 15.12X,F10.3,6X,10(1X 17.2))
RETURN
END

```

```

C
C      FIBONACCI SEARCH FUNCTION
C

```

```

DOUBLE PRECISION FUNCTION FIBON( DOUND )
DOUBLE PRECISION RATIO, FIB(50),
5 LBOUND, HBOUND, TNTRP, FINTR, DELTA, TESTLH
7, TESTRH, TLHV, THHV, TEST, FACT, TLH ,F
9, INTEGER EXCHT, EXPNO, FLAG

```

```

LBOUND = 0.0
TEST = 1.0
HBOUND = 1.0
FINTER = 0.0001
FACT = 1.618031

C DETERMINE THE INTERVALS OF THE FIBONACCI SEARCH
C

10 CONTINUE
TLBV = F ( TEST )
THBV = F ( HBOUND )
IF (TLBV GT THBV) GO TO 20
TLB = TEST
TEST = HBOUND
HBOUND= HBOUND * FACT
GO TO 10
20 CONTINUE

C DETERMINE POUNDS AND DELTA FOR FIBONACCI SEARCH
C

IF (TEST NE 1) LBOUND = TLB
INTER= HBOUND- LBOUND
DELTA = TEST - LBOUND
TESTLP= TEST
TESTHR= HBOUND - DELTA
IF (TESTLP LT TESTHR) GOTO 38
TLP = TESTLP
TESTLP = TESTHR
TESTHR = TLB
DELTA = TESTLP - LBOUND
TESTHR = HBOUND - DELTA
38 CONTINUE
INTER = HBOUND - LBOUND
RATIO = INTER/FINTER

C DETERMINE THE NUMBER OF EXPERIMENTS REQUIRED
C

FIBO(1) = 1
FIBO(2) = 2
DO 39 I =3,50
  FIBO(I) = FIBO(I-1) + FIBO(I-2)
  IF (FIBO(I) LT FAIL0) EXPNO = I + 1
39 CONTINUE

40 START CLOSED BOUND FIBONACCI EXPERIMENT
      IF (40 EXPNO=5, EXPNO
TLBV= I (TESTLP)
THBV= I (TESTHR)
IF (TLBV CF THBV) GO TO 10 30
LBOUND= TESTLP
INTER= HBOUND - LBOUND
LCTA= INTER- DELTA
TESTLP= TESTHR
TESTHR= HBOUND - DELTA
FLAG = 1
GO TO 40
30 CONTINUE

```

```

HBOUND= TESTHR
INTER= HBOUND - LBOUND
DELTA= INTER - DELTA
TESTLB= TESTLR
TESTLR= LBOUND + DELTA
FLAG = 0
40 CONTINUE
IF (FLAG EQ 1) FIBON = TESTLR
IF (FLAG EQ 0) FIBON = TESTHR
RETURN
END

C FUNCTION EVALUATION FOR FIBONACCI SEARCH
C

DOUBLE PRECISION FUNCTION F(I)
DOUBLE PRECISION K, TEST(20), X(20), S(20), FUNCT
COMMON X, S, NTERM
DO 10 J=1, NTERM
    TEST(J)=X(I) - K * S(1)
10 CONTINUE
F= -FUNCT( TEST )
RETURN
END

C CALCULATE VALUE OF ERROR FUNCTION
C

DOUBLE PRECISION FUNCTION FUNCT (X)
DOUBLE PRECISION X(20)
INTEGER STEP,COUNT
REAL GAM,P,CV,W,H,K1,K2,RADIUS,LENGTH,TNOT,TINF
REAL P0,RHO0,U0
COMPLEX PPG,RV,PP,UT
REAL PA(10),MAG
COMMON/RLOCK/STEP,COUNT,GAM,R,CV,W,H,K1,K2,FADIUS,LENGTH,TNOT,
&TINF,P0,RHO0,U0,PP0,PA,RV,RP,UT
REAL P(100),RHO(100),U(100),A0
COMPLEX UP(100),PP(100),UP0
REAL RZ, JP ,PHASE

RV = (1,0)* X(1) + (0,1) * X(2)
A0 = SQRT(GAM*P0/PH00)
UP0 = RV*A0*PP0/GAM/P0/100
CALL RFITOUR(GAM,P,CV,COUNT,H,W,K1,K2,FADIUS,LENGTH,F0,FH00,U0,
&A0,P0,PP0,P,RHO,U,UP,PP,TNOT,TINF)

OPTIM = 0.0
DO 747 N=1,10
    PZ = REAL (PP(N+1))
    IP = ATOMAG(IP(N+1))
    PHASE = ATAN ((IP/PZ)*180/PI 141576eE4
    IF ((PZ EQ 0) AND (IP EQ 0)) PHASE = 0
    IF ((PZ LT 0) AND (IP EQ 0)) PHASE = 180
    IF ((PZ EQ 0) AND (IP LT 0)) PHASE = -180
    IF ((PZ LT 0) AND (IP LT 0)) PHASE = PHASE+180
    MAG = PHASE
    OPTIM = OPTIM + (IA(N)-MAG)*K
747 CONTINUE

FUNCT = OPTIM
RETURN
END

```

```

C      READ RV-MEASUREMENT APPARATUS AND ENVIRONMENTAL DATA
C

SUBROUTINE INPUT

INTEGER STEP,COUNT
REAL GAM,R,CV,W,H,K1,K2,RADIUS,LENGTH,TNOT,TINF
REAL P0,RHO0,U0
COMPLEX PPO,RV,FP,UT
REAL PA(10)
COMMON/BLOCK/STEP,COUNT,GAM,R,CV,W,H,K1,K2,RADIUS,LENGTH,TNOT,
&TINF,P0,RHO0,U0,PPO,PA,RV,RP,U1

OPEN (UNIT = 3,FILE='INDAT ST',STATUS = 'OLD')

READ(3,*) GAM,R,CV,STEP,COUNT,H,W,K1,K2,RADIUS,LENGTH,P0,RHO0,P10
& RV,PP,UT ,U0,TNOT,TINF,FA(1),FA(2),FA(3),FA(4),FA(5)

RETURN
END

SUBROUTINE RKFOUR (GAM,R,CV,COUNT,H,W,K1,K2,RADIUS,LENGTH,P0,
&RHO0,U0,UP0,PF0,P,RHO,U,UP,PP,TNOT,TINF)
INTEGER COUNT
REAL GAM,R,CV,W,H,K1,K2,RADIUS,LENGTH,T1,T2
REAL P(100),RHO(100),U(100),P0,RHO0,U0
COMPLEX UP(100),PP(100),UF0,PP0
COMPLEX A1,A2,A3,A4,A5,P1,P2,P3,P4,P5,C1,C2,C3,C4,C5,D1,D2,D3,
&D4,D5
COMPLEX FUNC1,FUNC2,FUNC3,FUNC4,FUNC5
REAL TDIST,TDERIV

C      BOUNDARY CONDITIONS AT PROPELLANT SURFACE
C

P(1) = P0
RHO(1) = RHO0
U(1) = U0
UF(1) = UP0
FF(1) = FP0

C      RUNGE-KUTTA FOURTH-ORDER INTEGRATION ALGORITHM
C

DO 1 N = 3,POINT-1

T1 = TNOT*(N,LENGTH),TNOT,TINF,P1,K2,RADIUS,LENGTH)
T2 = TDERIV(N,LENGTH,H,TNOT,TINF,K1,K2,RADIUS,LENGTH,H)

A1 = FUNC1 (P(N),RHO(N),U(N),UP(N),PP(N),T1,T2,GAM,F,CV,W)*H
A2 = FUNC2 (P(N),RHO(N),U(N),UP(N),PP(N),T1,T2,GAM,R,CV,W)*H
A3 = FUNC3 (P(N),RHO(N),U(N),UP(N),PP(N),T1,T2,GAM,F,CV,W)*H
A4 = FUNC4 (P(N),RHO(N),U(N),UP(N),PP(N),T1,T2,GAM,R,CV,W)*H
A5 = FUNC5 (P(N),RHO(N),U(N),UP(N),PP(N),T1,T2,GAM,R,CV,W)*H

P1 = FUNC1 (P(N) + A1/2,RHO(N) + A2/2,U(N) + A3/2,UP(N) + A4
&/2,PP(N) + A5/2,T1,T2,GAM,R,CV,W)*H
B2 = FUNC2 (P(N) + A1/2,RHO(N) + A2/2,U(N) + A3/2,UP(N) + A4
&/2,PP(N) + A5/2,T1,T2,GAM,R,CV,W)*H

```

```

B3 = FUNC3 (P(N) + A1/2,RHO(N) + A2/2,U(N) + A3/2,UP(N) + A4
$/2,PP(N) + A5/2,T1,T2,GAM,R,CV,W) *H
B4 = FUNC4 (P(N) + A1/2,RHO(N) + A2/2,U(N) + A3/2,UP(N) + A4
$/2,PP(N) + A5/2,T1,T2,GAM,R,CV,W) *H
B5 = FUNC5 (P(N) + A1/2,RHO(N) + A2/2,U(N) + A3/2,UP(N) + A4
$/2,PP(N) + A5/2,T1,T2,GAM,R,CV,W) *H

C1 = FUNC1 (P(N) + B1/2,RHO(N) + B2/2,U(N) + B3/2,UP(N) + B4
$/2,PP(N) + B5/2,T1,T2,GAM,R,CV,W) *H
C2 = FUNC2 (P(N) + B1/2,RHO(N) + B2/2,U(N) + B3/2,UP(N) + B4
$/2,PP(N) + B5/2,T1,T2,GAM,R,CV,W) *H
C3 = FUNC3 (P(N) + B1/2,RHO(N) + B2/2,U(N) + B3/2,UP(N) + B4
$/2,PP(N) + B5/2,T1,T2,GAM,R,CV,W) *H
C4 = FUNC4 (P(N) + B1/2,RHO(N) + B2/2,U(N) + B3/2,UP(N) + B4
$/2,PP(N) + B5/2,T1,T2,GAM,R,CV,W) *H
C5 = FUNC5 (P(N) + B1/2,RHO(N) + B2/2,U(N) + B3/2,UP(N) + B4
$/2,PP(N) + B5/2,T1,T2,GAM,R,CV,W) *H

D1 = FUNC1 (P(N) + C1,RHO(N) + C2,U(N) + C3,UP(N) + C4,PP(N)
+ C5,T1,T2,GAM,R,CV,W) *H
D2 = FUNC2 (P(N) + C1,RHO(N) + C2,U(N) + C3,UP(N) + C4,PP(N)
+ C5,T1,T2,GAM,R,CV,W) *H
D3 = FUNC3 (P(N) + C1,RHO(N) + C2,U(N) + C3,UP(N) + C4,PP(N)
+ C5,T1,T2,GAM,R,CV,W) *H
D4 = FUNC4 (P(N) + C1,RHO(N) + C2,U(N) + C3,UP(N) + C4,PP(N)
+ C5,T1,T2,GAM,R,CV,W) *H
D5 = FUNC5 (P(N) + C1,RHO(N) + C2,U(N) + C3,UP(N) + C4,PP(N)
+ C5,T1,T2,GAM,R,CV,W) *H

F (N+1) = F (N) + 1 /6 *(A1 + 2*B1 + 2*C1 + D1)
RHO (N+1) = RHO (N) + 1 /6 *(A2 + 2*B2 + 2*C2 + D2)
U (N+1) = U (N) + 1 /6 *(A3 + 2*B3 + 2*C3 - D3)
UP (N+1) = UP (N) + 1 /6 *(A4 + 2*B4 + 2*C4 + D4)
PP (N+1) = PP (N) + 1 /6 *(A5 + 2*B5 + 2*C5 + D5)

1 CONTINUE
RETURN
END

C
C FUNCTION FUNC 1 THRU 5 ARE GOVERNING EQUATIONS IN RK FORM
C

COMPLEX FUNCTION FUNC1 (A,B,C,D,E,F,G,H,I,J,L)
REAL A,B,C,F,G,H,I,J,K
COMPLEX D,E
FUNC1 = 0
RETURN
END

COMPLEX FUNCTION FUNC2 (A,B,C,D,E,F,G,H,I,J,L)
REAL A,B,C,F,G,H,I,J,K
COMPLEX D,F
FUNC2 = -F*F*G
RETURN
END

COMPLEX FUNCTION FUNC3 (A,B,C,D,E,F,G,H,I,J,L)
REAL A,B,C,F,G,H,I,J,K
COMPLEX D,F
FUNC3 = F*G*F*G
RETURN
END

COMPLEX FUNCTION FUNC4 (A,B,C,D,E,F,G,H,I,J,L)
REAL A,B,C,F,G,H,I,J,K
COMPLEX D,E

```

```

COMPLEX FUNC3,L
L = FUNC3 (A,B,C,D,E,F,G,H,I,J,K)
FUNC4 = (1/(B*C*C - H*A))*(0,1.)*K*K + (C/(B*C*C - H*A))*B*B
*(G,1)*K*K*D + (1/(H*C*C - H*A))*(H*A - P*D*C)*L
RETURN
END

COMPLEX FUNCTION FUNC5 (A,H,C,D,E,F,G,H,I,J,K)
REAL A,B,C,F,G,H,I,J,K
COMPLEX D,E
COMPLEX FUNC3,L ,FUNC4,M
L = FUNC3 (A,B,C,D,E,F,G,H,I,J,K)
M = FUNC4 (A,H,C,D,E,F,G,H,I,J,K)
FUNC5 = -B*B*(0,1)*K*K*D - P*D*C*M - B*D*I
RETURN
END

C
C      FUNCTION TDIST CALCULATES TEMPERATURE ALONG AXIS
C

REAL FUNCTION TDIST (N,LENGTH,TNOT,F1,F2,RADIUS)
INTEGER N
REAL LENGTH,TNOT,K1,K2,RADIUS,LAMDA,DIST,VALUE
LAMDA = 2*K2/K1/RADIUS/LENGTH
DIST = N/100*LENGTH
VALUE = (TNOT - TINF)*EXP(-LAMDA*DIST)+TINF
TDIST = VALUE
RETURN
END

C
C      FUNCTION TDERRIV CALCULATES TEMP GRADIENT ALONG AXIS
C

REAL FUNCTION TDERRIV (N,LENGTH,TNOT,F1,F2,RADIUS)
INTEGER N
REAL LENGTH,TNOT,F1,K2,RADIUS,LAMDA,DIST,VALUE
LAMDA = 2*K2/K1/RADIUS/LENGTH
DIST = N/100*LENGTH
VALUE = -LAMDA*(TNOT - TINF)*EXP(-LAMDA*DIST)
TDERRIV = VALUE
RETURN
END

```

Appendix 3: Admittance to Rv Conversion

This appendix contains a listing of the program which is used to convert admittance values to velocity-coupled response function values.

Program 2

```
FTN7X

C      ADMITTANCE TO VELOCITY-COUPLED RESPONSE FUNCTION CONVERSION
C

PROGRAM ADRV
REAL A,U,GAM,P0,UT
COMPLEX AB,PP,RP,RV
GAM = 1.4
P0 = 101300
U = 6.0
A = SQRT(GAM*P0/1.224)
UT=19
WRITE (1,*)
WRITE (1,*) 'ADMITTANCE-RV CONVERSION'
WRITE (1,*) -----
WRITE (1,*) ''
WRITE (1,*) 'INPUT PRESSURE-COUPLED RESPONSE FUNCTION VALUE'
READ (1,*) RP
WRITE (1,*) ''
WRITE (1,*) 'INPUT ADMITTANCE VALUE'
READ (1,*) AB
PP = (0.,1200.)
RV = A/U/UT * (AI*A*FP/GAM/P0 - U*FP/GAM/P0 *(RF-1))
WRITE (1,*)
WRITE (1,*) 'RV VALUE IS ',RV
END
```

CI.42> ADRV

ADMITTANCE-RV CONVERSION

INPUT PRESSURE-COUPLED RESPONSE FUNCTION VALUE
(0.1,-0.1)

INPUT ADMITTANCE VALUE
(0.00,0.02)

RV VALUE IS (- 18716,.13643)

CI.42> ADRV

ADMITTANCE-RV CONVERSION

INPUT PRESSURE-COUPLED RESPONSE FUNCTION VALUE
(0.1,-0.1)

INPUT ADMITTANCE VALUE
(0.04,-0.02)

RV VALUE IS (.15684,.48043)

Appendix 4: Gaussian Random Number Generator

This program was used to generate the random numbers that were used to simulate experimental data. A listing of the random numbers that were used in the testing of the program is included.

Program 3

```
FIN7X

C      RANDOM NUMBER GENERATOR - SAMPLING FROM GAUSSIAN DIST
C

PROGRAM GAUSS

REAL R

WRITE (6,*) 'GAUSSIAN RANDOM NUMBER GENERATOR'
WRITE (6,*)
DO 100 I=1,5
    WRITE (6,*) 'STANDARD DEVIATION = ,1
    DO 200 N = 1,10
        R = 1*GRAN (1)
        WRITE (6,300) R
300 FORMAT ('    R = ',F6 .3)
200 CONTINUE
WRITE (6,*)
100 CONTINUE
END
```

GAUSSIAN RANDOM NUMBER GENERATOR

STANDARD DEVIATION = 1

R = 402
R = 121
R = -1 409
R = 929
R = 700
P = -291
R = 1 026
R = 2 833
R = 473
R = 558

STANDARD DEVIATION = 2

R = 3 156
R = 2 636
R = -1 319
R = 2 598
R = -4 476
R = 416
R = 195
R = 973
R = 1 230
R = 2 022

STANDARD DEVIATION = 3

P = -3 196
P = -2 285
R = 3 671
R = 138
R = 4 287
R = 007
R = 5 532
R = 3 495
R = 963
P = -3 174

STANDARD DEVIATION = 4

P = 4 102
P = 3 252
P = -2 328
R = -690
R = 471
R = 4 639
R = 1 001
R = 4 078
R = 1 057
R = -3 559

STANDARD DEVIATION = 5

P = -3 955
P = 017
P = -413
P = -1 514
R = -9 059
R = -7 215
R = -1 709
R = 1 760
R = -6 044
R = 8 231

Appendix 5: Parametric Studies

The following figures show how the pressure phase angle distribution within the Rv-measurement apparatus varies with the real and imaginary components of the admittance value for a solid propellant for conditions specified in appendix 1. Figures A.1 through A.5 show the phase angle distribution dependence on the real component of the admittance when the imaginary component is held fixed. Figures A.6 through A.10 show a similar dependence when the real component is held fixed. From the figures presented here it can be seen that the phase angle distribution is slightly more sensitive to variations in the real component of the admittance. Consequently, better performance of the curve-fit procedure can be expected for the real component of the admittance than for the imaginary component.

The apparent discontinuity in the curves of figures A.2 through A.10 results from the choice of scale. The curves cross the 180 degree line which is equivalent to the -180 line. These curves have the same form as the curve in figure A.1.

Whereas, the figures show the phase angle distributions at the location nearest the propellant sample where variation is greatest, the tabulated results are provided to show how both magnitude and phase angle components of the pressure vary throughout the length of the Rv-measurement apparatus. The magnitude of the pressure is provided in decibel units as well as Pascals units for convenience.

A typical plot of the magnitude component of the

perturbation pressure distribution is provided in figure A.11. This plot reveals the severe non-linearity at very low pressures which prevents effective use of magnitude information in numerical curve-fit procedures.

PRESSURE PHASE VS. DISTANCE

admittance = (0.04, -0.02)

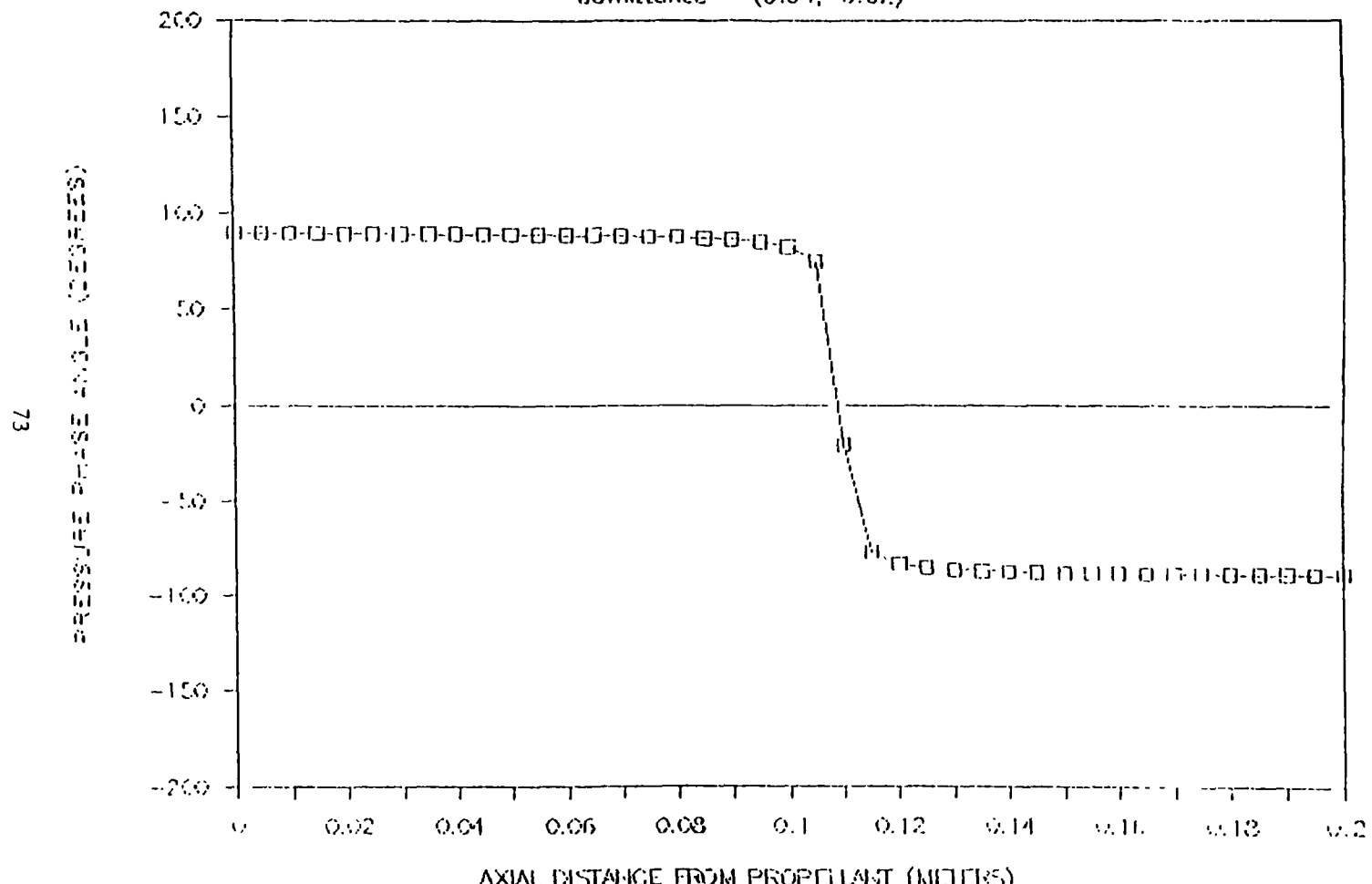


Figure A.1

PRESSURE PHASE VS. DISTANCE

admittance = $(v_{CO_2} - v_{CO})$

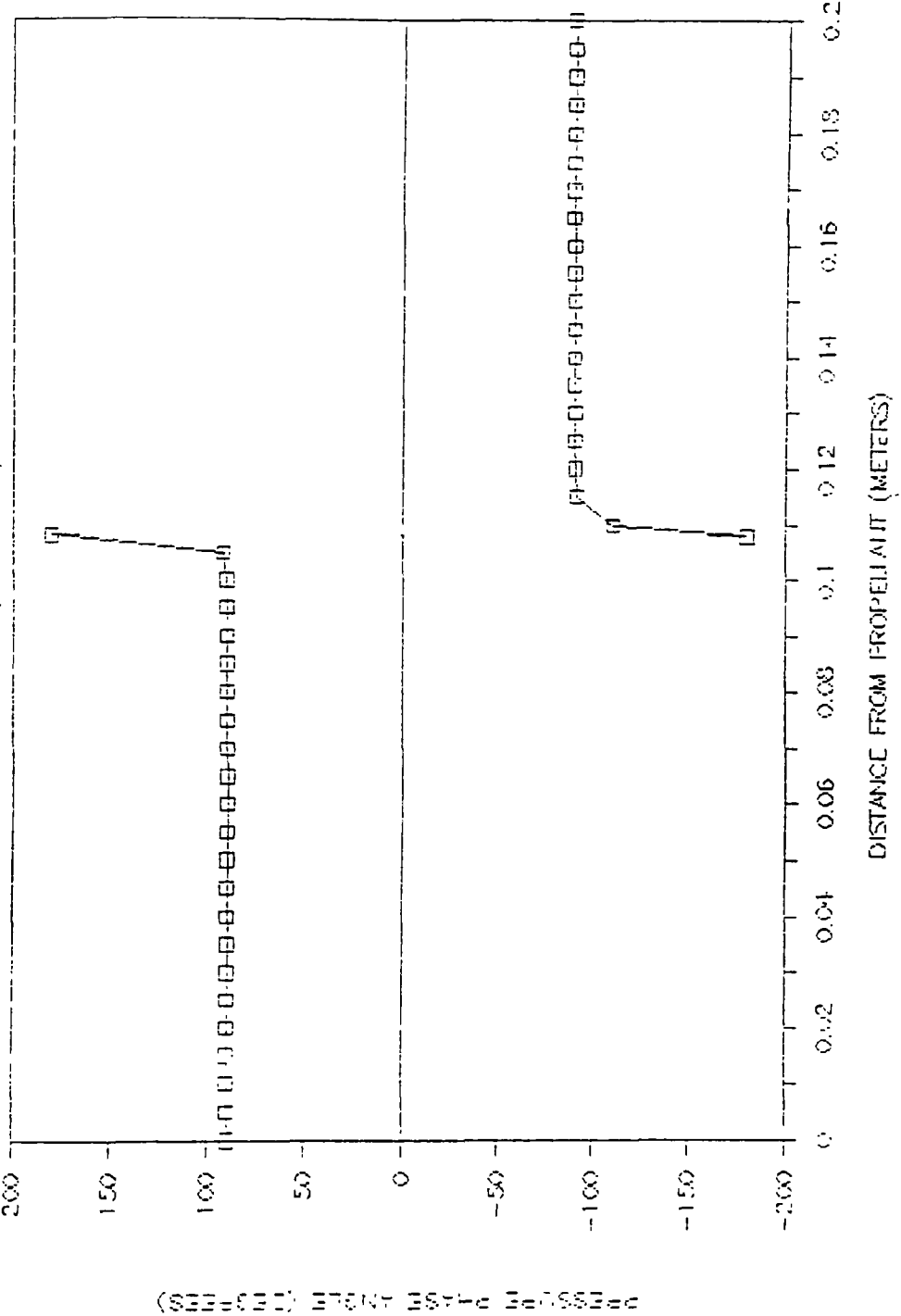


Figure A.2

PRESSURE PHASE VS. DISTANCE

admittance = (0.00,-0.02)

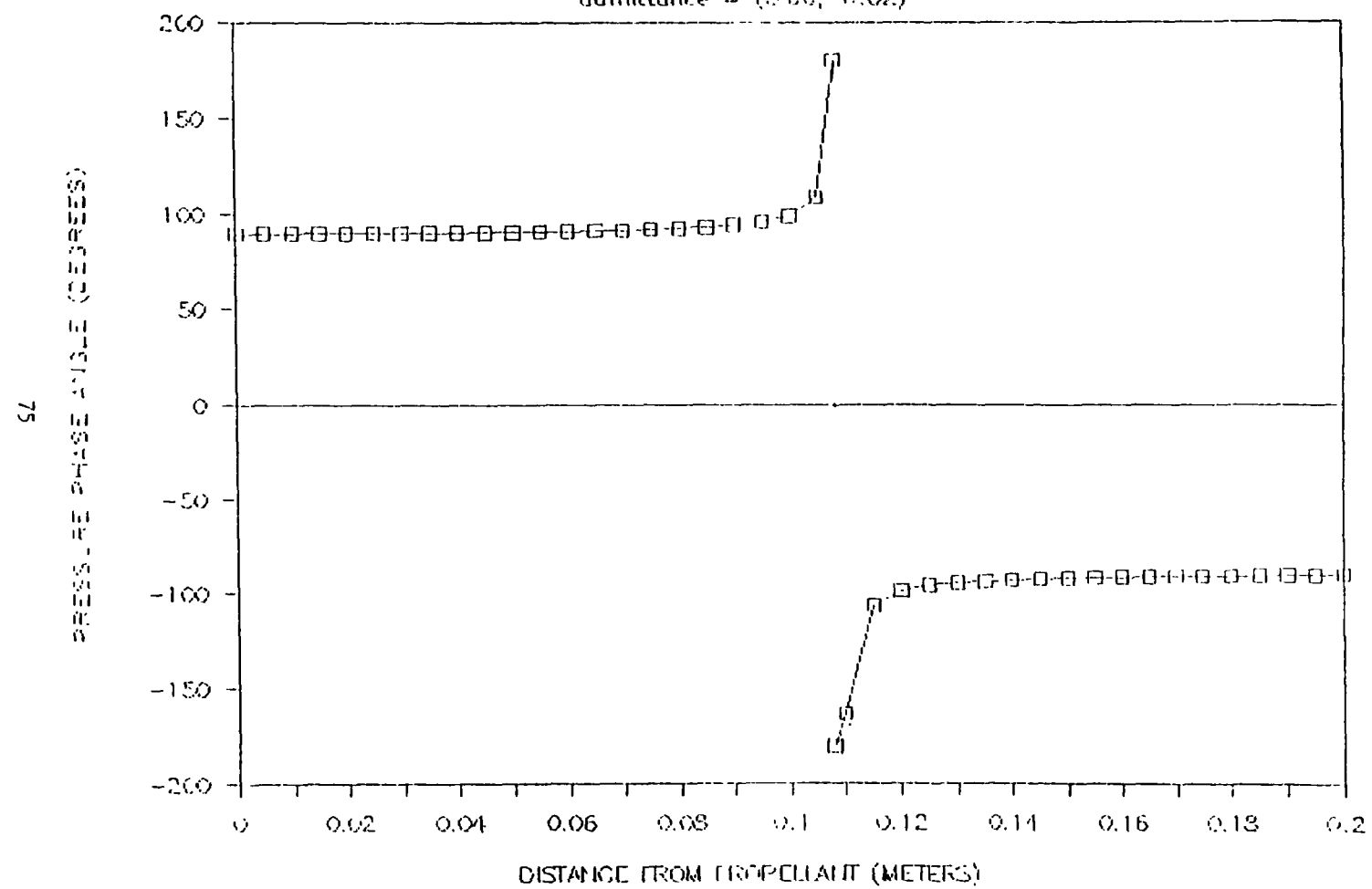


Figure A.3

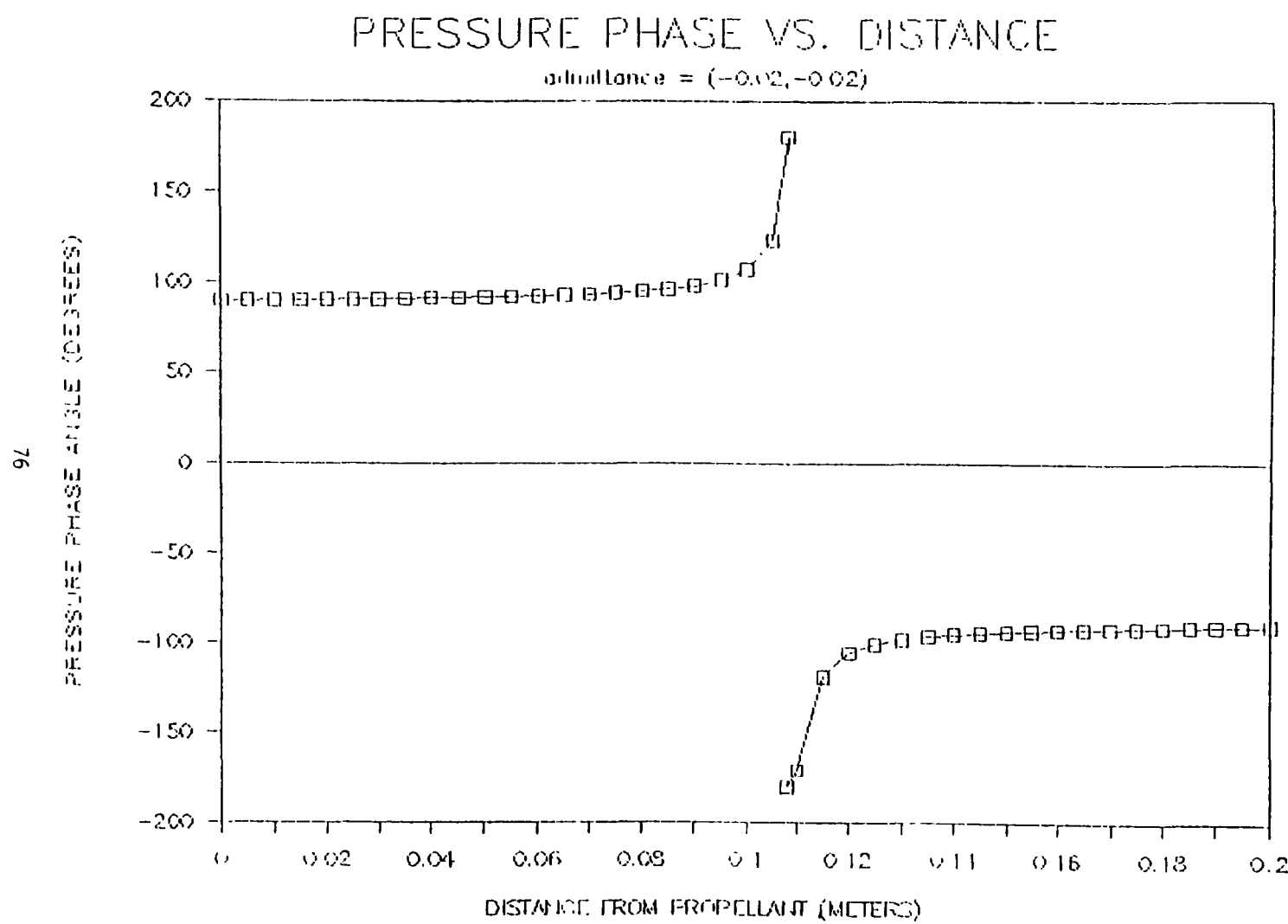


Figure A.4

PRESSURE PHASE VS. DISTANCE

admittance = (-0.01,-0.02)

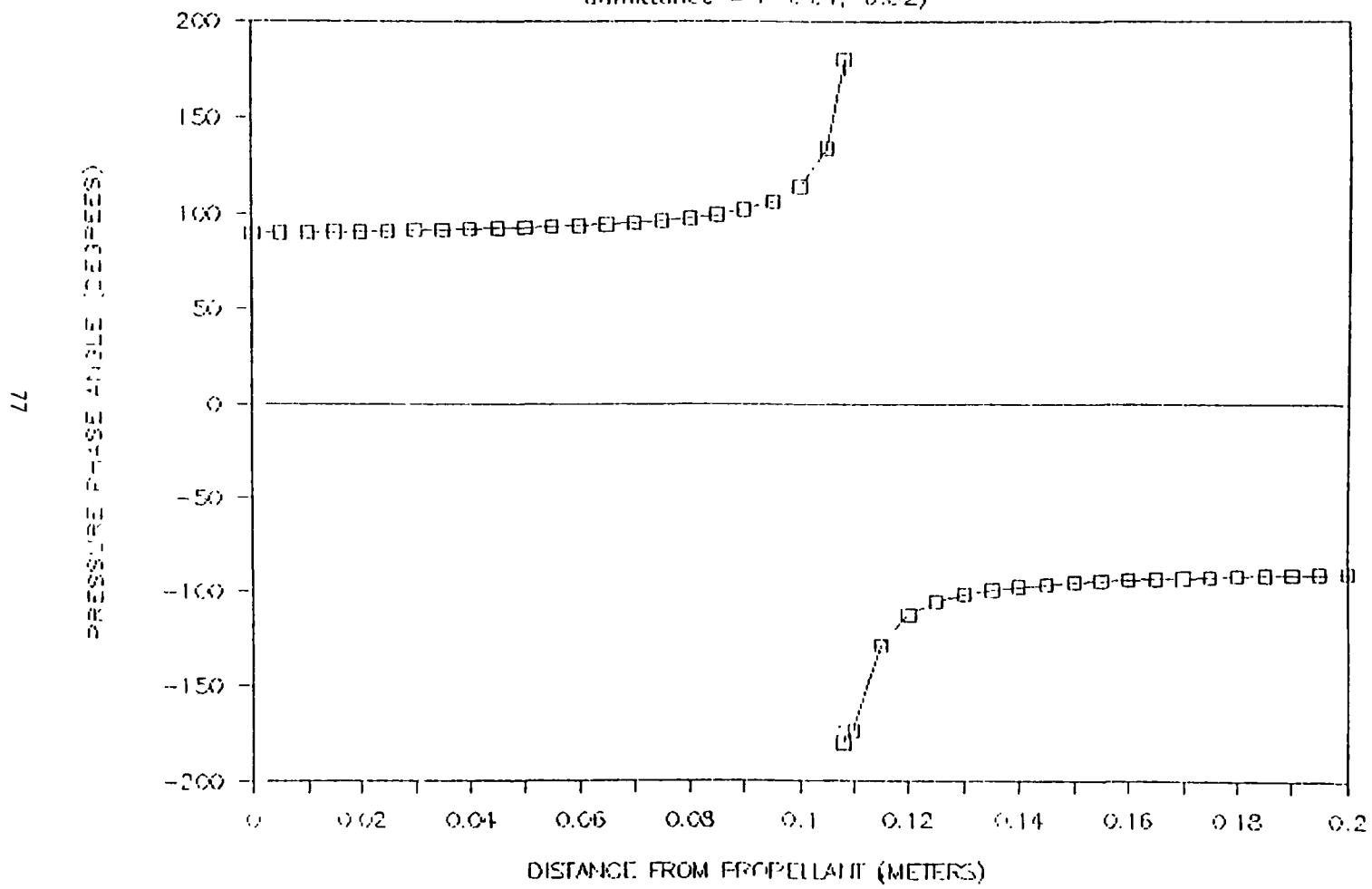


Figure A.5

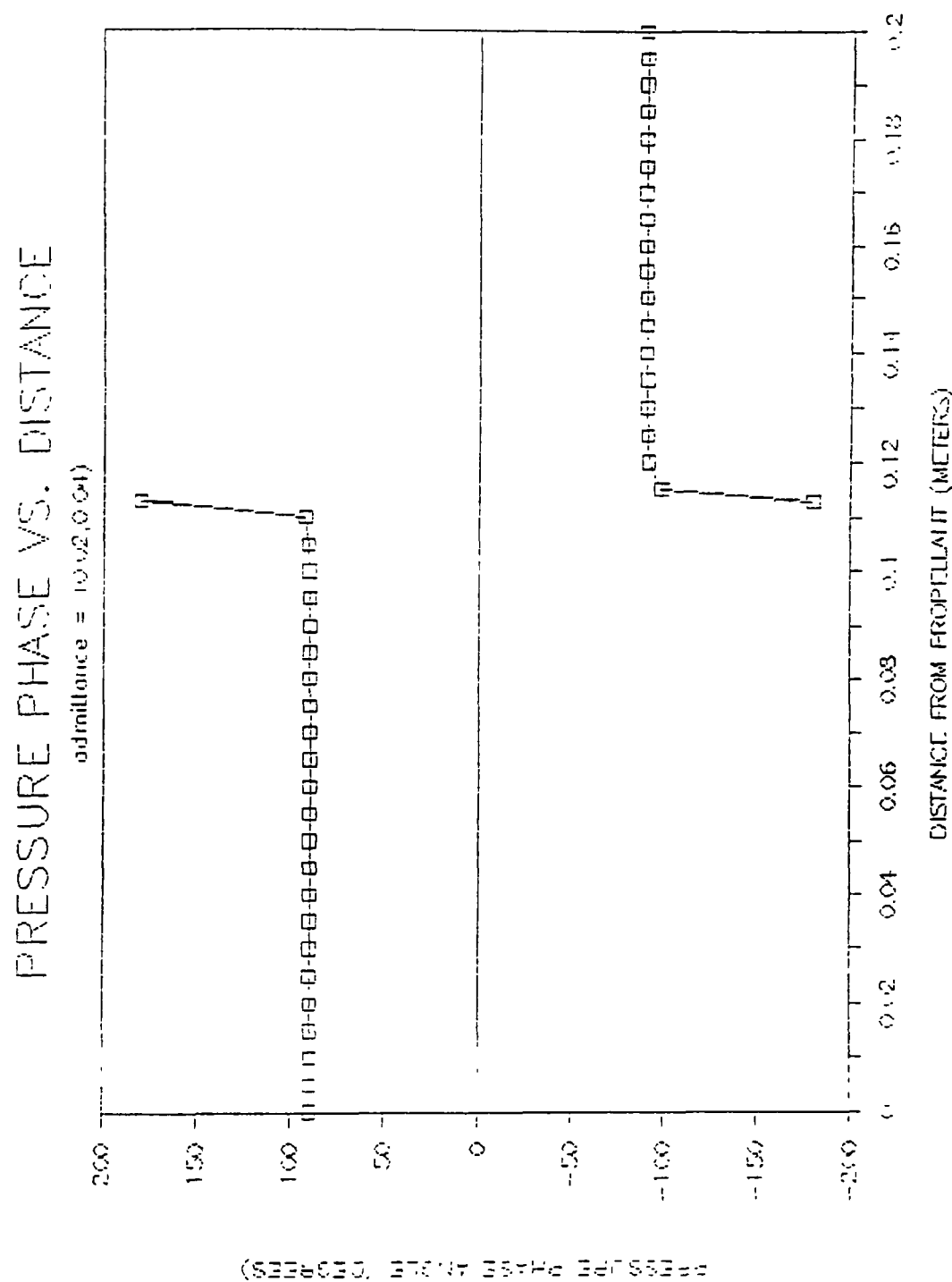


Figure A.6

PRESSURE PHASE VS. DISTANCE

admittance = 0.02, 0.02)

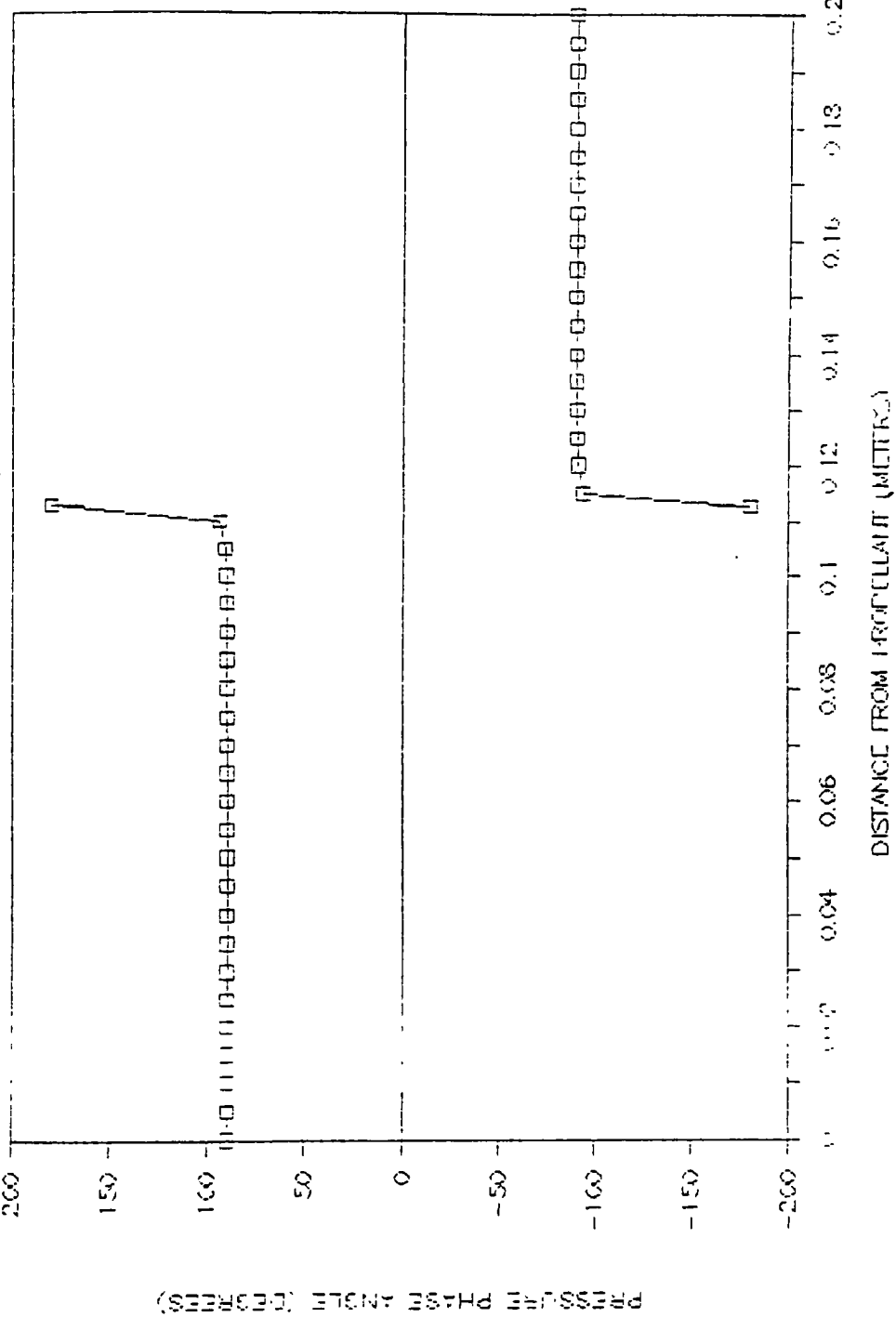


Figure A.7

PRESSURE PHASE VS. DISTANCE

admittance = (1.02,0.00)

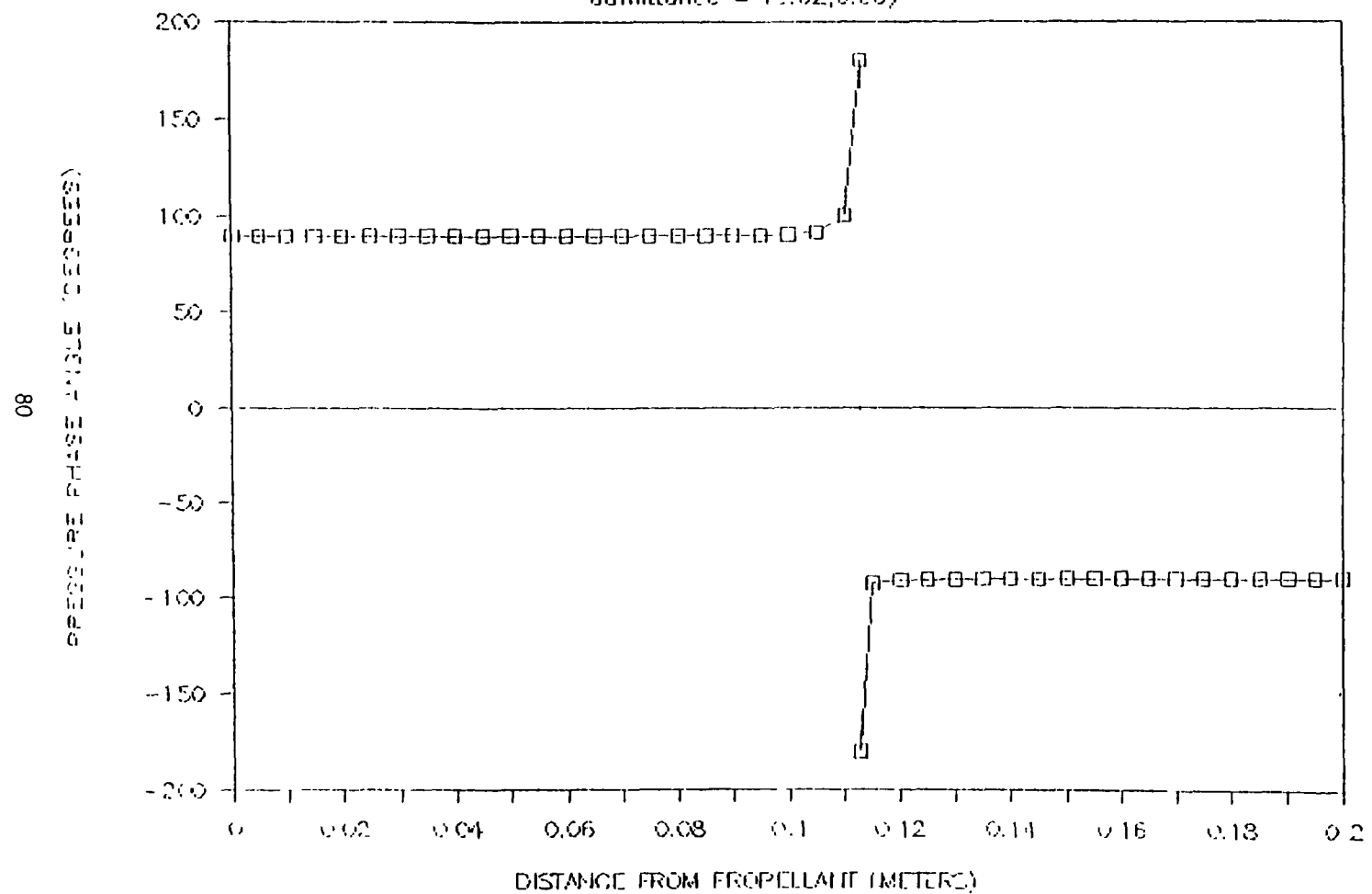


Figure A.8

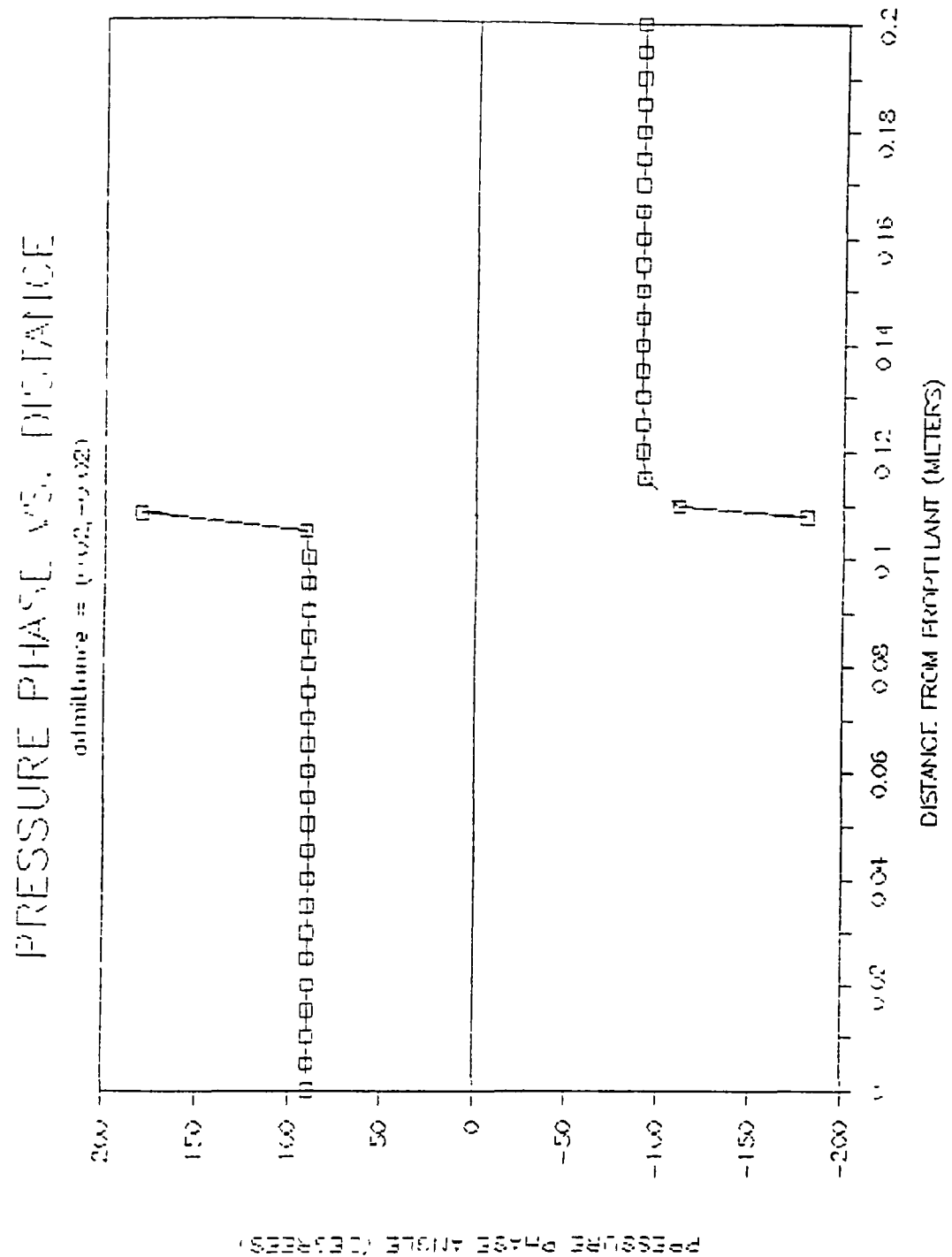


Figure A.9

PRESSURE PHASE VS. DISTANCE

admittance = (0.02,-0.01)

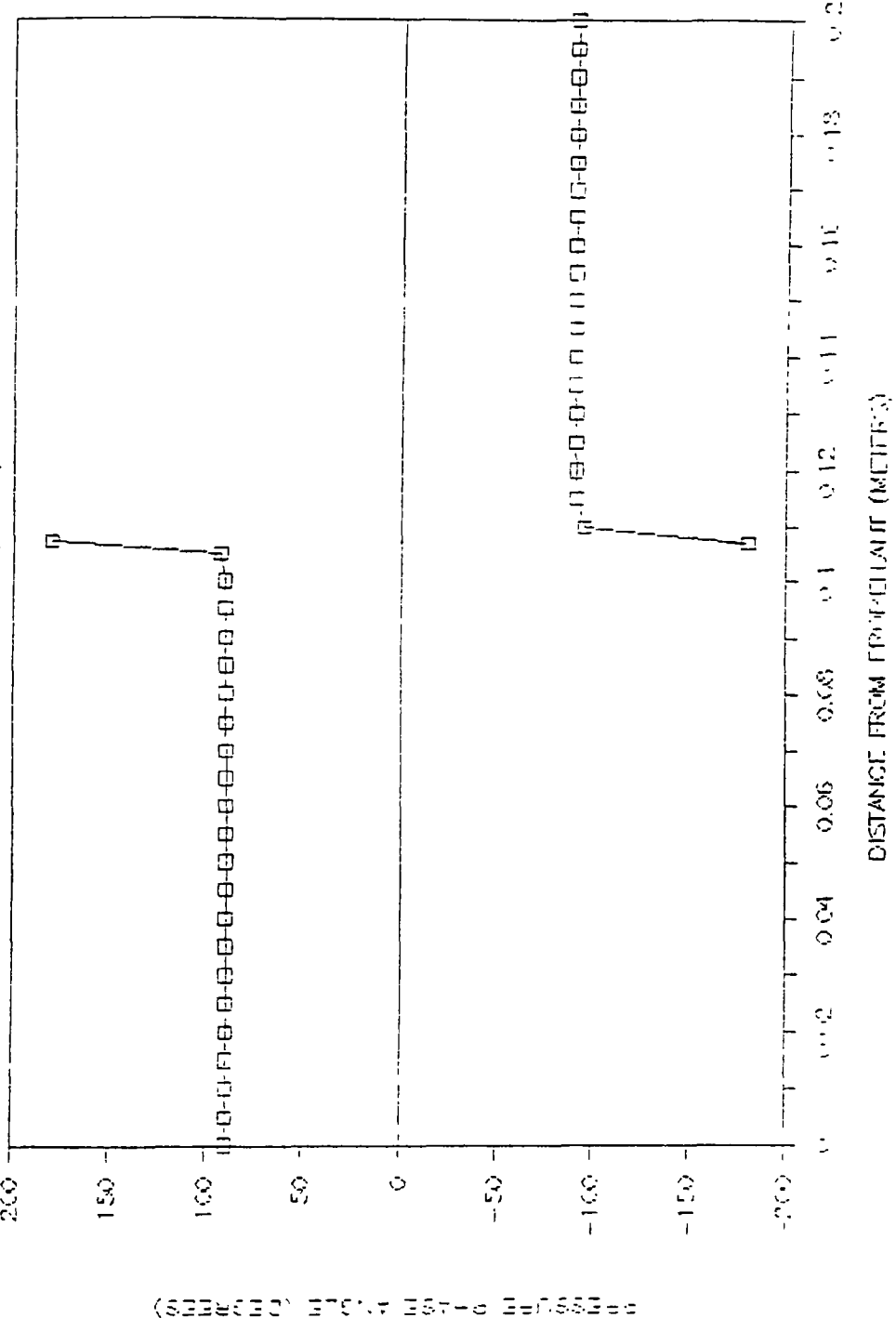


Figure A.10

PRESSURE MAGNITUDE VS. DISTANCE.

admittance = $(W_{\lambda_2} - \alpha \cdot \phi)$

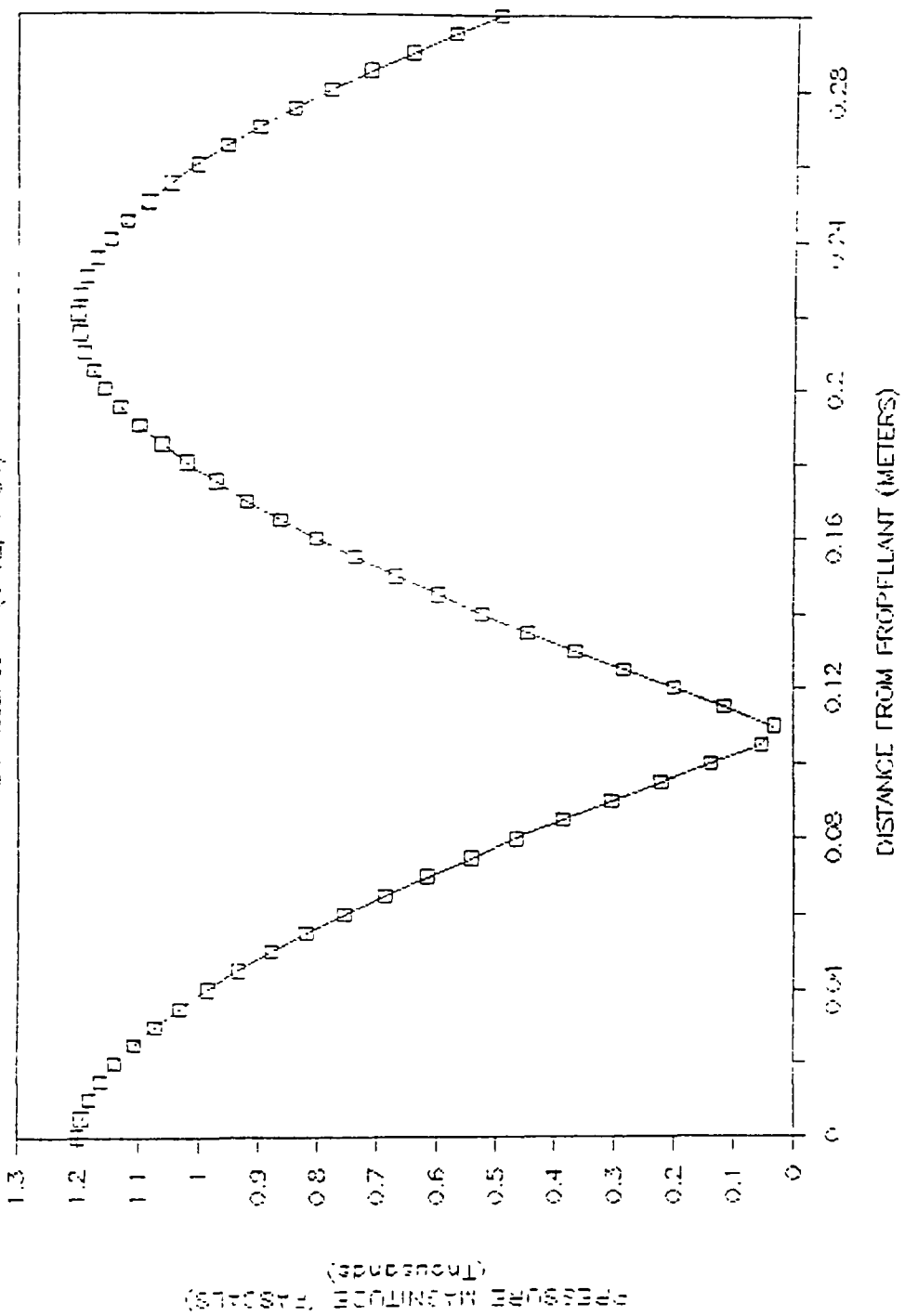


Figure A.11

ADMITTANCE = (4 E-2,-2 E-2)

ITERATION	DISTANCE	PRESSURE DISTRIBUTION		PRESSURE
		MAG(db)	PHASE	
0	0 000	152 467	90 000	1200 010
1	305	152 433	89 929	1195 290
2	610	152 355	89 857	1194 609
3	915	152 232	89 784	1167 987
4	1220	152 063	89 708	1145 515
5	1525	151 847	89 628	1117 306
6	1830	151 580	89 544	1083 510
7	2135	151 259	89 454	1044 264
8	2440	150 881	89 357	999 808
9	2745	150 441	89 250	950 340
10	3050	149 930	89 130	876 115
11	3355	149 342	88 994	837 405
12	3660	148 664	88 828	774 504
13	3965	147 880	88 652	707 730
14	4270	146 972	88 486	637 418
15	4575	145 908	88 143	563 925
16	4880	144 645	87 773	487 625
17	5185	143 116	87 263	408 910
18	5490	141 206	86 505	328 194
19	5795	138 699	85 344	245 928
20	6100	135 109	82 700	162 671
21	6405	128 901	74 816	79 593
22	6710	117 902	-31 187	22 436
23	7015	130 466	-77 341	95 307
24	7320	135 922	-83 329	178 616
25	7625	139 240	-85 506	261 739
26	7930	141 608	-86 637	343 746
27	8235	143 433	-87 335	424 113
28	8540	144 904	-87 813	502 399
29	8845	146 125	-89 163	578 193
30	9150	147 156	-88 433	651 106
31	9455	148 039	-88 650	720 769
32	9760	148 801	-88 820	786 829
33	10065	149 461	-88 582	848 953
34	10370	150 034	-89 114	906 839
35	10675	150 530	-89 331	960 365
36	10980	150 950	-89 726	1048 645
37	11285	151 325	-89 432	1052 573
38	11590	151 675	-89 531	1040 363
39	11895	151 892	-89 604	1123 152
40	12200	151 099	-89 682	1158 255
41	12505	152 259	-89 758	1171 618
42	12810	152 373	-89 831	1187 111
43	13115	152 443	-89 903	1196 661
44	13420	152 468	-89 974	1200 215
45	13725	152 450	-90 044	1197 756
46	14030	152 389	-90 116	1189 303
47	14335	152 262	-90 189	1174 888
48	14640	152 172	-90 264	1154 550
49	14945	151 433	-90 342	1128 349
50	15250	151 685	-90 424	1090 776
51	15555	151 325	-90 501	1059 550
52	15860	151 070	-90 606	1017 110
53	16165	150 613	-90 709	969 394
54	16470	150 130	-90 824	916 916
55	16775	149 572	-90 953	859 848
56	17080	148 928	-91 101	798 477
57	---	---	-	---

57	285	148.186	-71.279	733 111
58	290	147.328	-91.484	664 081
59	295	146.326	-91.743	591 734
60	300	145.143	-92.076	516 438
61	305	143.724	-92.525	438 577
62	310	141.974	-93.172	358 559
63	315	139.727	-94.197	276 015
64	320	136.632	-96.694	193 849
65	325	131.746	-100.852	110 443
66	330	120.865	-131.487	31 557
67	335	127.111	108.834	64 776
68	340	134.254	98.116	147 424
69	345	128.147	95.134	230 770
70	350	140.802	93.716	213 272
71	355	142.800	92.893	294 307
72	360	144.288	92.147	473 419
73	365	145.653	91.957	550 190
74	370	146.790	91.660	624 224
75	375	147.725	91.426	655 144
76	380	148.529	91.234	763 590
77	385	149.225	91.072	636 323
78	390	149.629	90.933	625 721
79	395	150.253	90.811	540 786
80	400	150.006	90.702	901 142
81	405	151.195	90.603	1036 534
82	410	151.525	90.512	1076 737
83	415	151.202	90.437	1111 546
84	420	152.037	90.347	1141 769
85	425	152.205	90.270	1164 318
86	430	152.336	90.196	1162 016
87	425	152.422	90.124	1192 793
88	440	152.464	90.053	1199 551
89	445	152.462	89.982	1199 320
90	450	152.417	89.911	1193 162
91	455	152.328	89.835	1180 567
92	460	152.154	89.765	1162 058
93	465	152.012	89.688	1138 923
94	470	151.784	89.607	1109 285
95	475	151.504	89.522	1074 091
96	480	151.169	89.430	1033 518
97	485	150.776	89.331	987.770
98	490	150.319	89.221	537 076
99	495	149.789	89.098	861 590
100	500	149.179	88.957	811 892

ADMITTANCE (2.E-2,-2 E-2)

PRESSURE DISTRIBUTION

ITERATION	DISTANCE	MAG(db)	PHASE	PRESSURE
0	0 000	152.467	<0 000	1200 000
1	005	152.433	>0 010	1195 297
2	010	152.355	<0 021	1184 606
3	015	152.232	>0 032	1167 979
4	020	152.063	<0 043	1145 500
5	025	151.646	>0 054	1117 282
6	030	151.570	<0 067	1083 467
7	035	151.259	>0 080	1044 322
8	040	150.891	<0 094	999 746
9	045	150.440	>0 110	950 261
10	050	149.929	<0 127	896 014
11	055	149.341	>0 147	837 279
12	060	148.662	<0 170	774 340
13	065	147.878	>0 197	707 538
14	070	146.968	<0 230	637 183
15	075	145.903	>0 272	563 636
16	080	144.838	<0 316	487 265
17	085	143.106	>0 401	408 453
18	090	141.190	<0 512	327 596
19	095	138.670	>0 697	245 100
20	100	135.140	<1 074	161 380
21	105	128.590	>2 274	76 875
22	110	109.640	-110 678	8 667
23	115	130.257	-91 883	93 041
24	120	135.864	-90 980	177 433
25	125	139.214	-90 659	260 952
26	130	141.593	-90 493	343 167
27	135	143.424	-90 390	423 665
28	140	144.898	-90 330	502 041
29	145	146.120	-90 269	577 902
30	150	147.153	-90 239	650 868
31	155	148.037	-90 198	720 573
32	160	148.799	-90 171	796 668
33	165	149.459	-90 149	848 822
34	170	150.033	-90 130	906 723
35	175	150.527	-90 113	960 081
36	180	150.958	-90 097	1018 628
37	185	151.324	-90 063	1052 123
38	190	151.634	-90 070	1090 345
39	195	151.893	-90 058	1123 105
40	200	152.098	-90 046	1150 228
41	205	152.259	-90 035	1171 607
42	210	152.373	-90 025	1187 107
43	215	152.443	-90 014	1196 658
44	220	152.468	-90 004	1200 215
45	225	152.450	-89 994	1197 757
46	230	152.389	-89 983	1185 299
47	235	152.283	-89 972	1174 882
48	240	152.132	-89 961	1154 578
49	245	151.973	-89 950	1136 480
50	250	151.807	-89 938	1116 746
51	255	151.683	-89 925	1097 507
52	260	151.629	-89 911	1016 562
53	265	150.612	-89 895	969 301
54	270	150.539	-89 880	916 827
55	275	149.570	-89 861	859 731
56	280	148.927	-89 839	798 332
57	-	-	--	--

57	285	148 184	-87 813	732 733
58	290	147 325	-89 783	663 862
59	295	146 322	-89 745	571 466
60	300	145 138	-89 696	516 106
61	305	143 716	-89 630	438 160
62	310	141 961	-89 535	258 020
63	315	139 704	-89 385	276 088
64	320	136 564	-89 105	192 777
65	325	131 592	-86 393	108 510
66	330	118 428	-82 628	23 836
67	335	125 644	87 143	61 384
68	340	134 169	88 805	145 880
69	345	138 113	89 248	239 877
70	350	140 754	89 456	212 618
71	355	142 789	89 576	267 215
72	360	144 381	89 656	473 031
73	365	145 686	89 714	540 677
74	370	146 786	89 757	623 968
75	375	147 723	89 791	694 933
76	380	148 527	89 819	762 417
77	385	149 224	89 643	826 081
78	390	149 826	89 863	865 616
79	395	150 332	89 881	840 884
80	400	150 805	89 897	891 160
81	405	151 194	89 912	1036 478
82	410	151 525	89 925	1076 884
83	415	151 801	89 938	1111 516
84	420	152 127	89 949	1140 768
85	425	152 204	89 961	1164 305
86	430	152 335	89 971	1182 069
87	435	152 422	89 982	1193 720
88	440	152 464	89 993	1190 590
89	445	152 462	90 003	1190 370
90	450	152 417	90 112	1197 166
91	455	152 228	90 024	1160 962
92	460	152 194	90 034	1162 647
93	465	152 013	90 046	1138 906
94	470	151 784	90 157	1119 259
95	475	151 364	90 070	1074 054
96	480	151 160	90 083	1033 468
97	485	150 776	90 098	987 703
98	490	150 250	90 114	936 770
99	495	149 786	90 132	981 583
100	500	149 578	90 152	821 778

ADMITTANCE = (0 E+0,-2 E-2)

ITERATION	DISTANCE	PRESSURE DISTRIBUTION		PRESSURE
		MAG(dB)	PHASE	
0	0 000	152 467	90 000	1200 000
1	005	152 433	90 092	1195 297
2	010	152 395	90 185	1184 612
3	015	152 332	90 280	1167 793
4	020	152 063	90 378	1145 525
5	025	151 847	90 481	1117 321
6	030	151 580	90 589	1083 523
7	035	151 260	90 706	1044 200
8	040	150 882	90 832	997 650
9	045	150 441	90 970	950 375
10	050	149 931	91 124	896 185
11	055	149 543	91 300	837 401
12	060	148 665	91 502	774 611
13	065	147 882	91 742	707 861
14	070	146 974	92 034	637 579
15	075	145 911	92 397	564 124
16	080	144 649	92 877	487 872
17	085	143 122	93 536	409 232
18	090	141 217	94 514	328 603
19	095	138 719	96 138	246 475
20	100	135 156	99 403	163 545
21	105	129 096	109 331	81 404
22	110	119 877	-163 308	28.230
23	115	130 603	-106 189	96 830
24	120	125 961	-98 597	177 423
25	125	129 258	-95 801	262 277
26	130	141 618	-94 343	344 142
27	135	143 437	-93 443	424 421
28	140	144 908	-92 226	502 644
29	145	146 128	-92 374	578 392
30	150	147 159	-92 025	651 369
31	155	148 041	-91 745	720 903
32	160	148 802	-91 513	786 939
33	165	149 462	-91 316	849 043
34	170	150 034	-91 145	906 501
35	175	150 531	-90 894	960 223
36	180	150 459	-90 859	1018 740
37	185	151 325	-90 734	1052 208
38	190	151 625	-90 620	1050 408
39	195	151 892	-90 512	1123 149
40	200	152 057	-90 410	1150 267
41	205	152 259	-90 313	1171 625
42	210	152 373	-90 218	1187 116
43	215	152 443	-90 126	1196 662
44	220	152 468	-90 034	1200 215
45	225	152 450	-89 943	1197 758
46	230	152 389	-89 850	1189 703
47	235	152 383	-89 754	1174 693
48	240	151 132	-89 655	1154 598
49	245	151 933	-89 556	1136 323
50	250	151 636	-89 453	1056 196
51	255	151 286	-89 331	1059 279
52	260	151 030	-89 237	1017 158
53	265	150 514	-89 023	969 444
54	270	150 130	-88 935	916 575
55	275	149 572	-88 769	859 926
56	280	148 929	-88 577	798 576

57	.285	148 188	-68 353	733 233
58	.290	147 329	-68 682	664 230
59	.295	146 328	-67 748	591 917
60	.300	145 147	-67 318	516 665
61	.305	143 730	-66 738	438 863
62	.310	141 983	-65 503	358 926
63	.315	139 743	-64 581	277 312
64	.320	126 665	-62 143	194 580
65	.325	121 648	-76 083	111 749
66	.330	121 986	-41 161	25 902
67	.335	127 405	66 208	67 001
68	.340	134 212	79 556	148 416
69	.345	122 170	63 389	231 305
70	.350	140 614	25 211	313 717
71	.355	142 807	26 264	354 643
72	.360	144 393	84 567	473 663
73	.365	145 697	67 472	550 405
74	.370	146 792	87 824	634 400
75	.375	147 736	88 157	695 268
76	.380	148 530	88 405	762 715
77	.385	149 226	88 614	826 319
78	.390	149 830	88 794	825 769
79	.395	150 253	89 952	840 644
80	.400	150 806	89 193	841 101
81	.405	151 155	89 221	1036 572
82	.410	151 526	89 338	1076 764
83	.415	151 602	89 448	1111 566
84	.420	152 127	89 552	1140 612
85	.425	152 205	89 651	1164 336
86	.430	152 336	89 747	1182 130
87	.435	152 422	89 840	1193 754
88	.440	152 464	89 933	1196 550
89	.445	152 462	90 023	1199 379
90	.450	152 417	90 115	1197 163
91	.455	152 326	90 203	1180 660
92	.460	152 154	90 304	1162 663
93	.465	152 013	90 403	1138 924
94	.470	151 764	90 508	1119 302
95	.475	151 504	90 618	1074 115
96	.480	151 170	90 718	1033 552
97	.485	150 777	90 865	987 814
98	.490	150 219	91 107	937 123
99	.495	140 780	91 166	881 763
100	.500	140 980	91 348	631 952

ADMITTANCE (-2.E-2,-2 E-2)

PRESSURE DISTRIBUTION				
ITERATION	DISTANCE	MAG(db)	PHASE	PRESSURE
0	0 000	152 467	90 000	1200 000
1	005	152 433	90 173	1195 303
2	010	152 355	90 348	1184 628
3	015	152 232	90 528	1168 929
4	020	152 064	90 713	1145 589
5	025	151 847	90 907	1117 422
6	030	151 581	91 112	1083 670
7	035	151 261	91 331	1044 503
8	040	150 884	91 569	1000 120
9	045	150 444	91 830	950 744
10	050	149 935	92 121	896 626
11	055	149 348	92 451	838 043
12	060	148 672	92 833	775 292
13	065	147 892	93 265	708 692
14	070	146 988	93 833	638 606
15	075	145 930	94 520	565 388
16	080	144 677	95 417	489 443
17	085	143 164	96 650	411 210
18	090	141 285	98 473	331 198
19	095	138 845	101 470	250 076
20	100	135 443	107 351	169 145
21	105	130 170	123 501	92 117
22	110	125 146	-170 970	51 660
23	115	131 392	-118 714	106 029
24	120	136 202	-105 921	184 483
25	125	139 370	-100 851	265 684
26	130	141 681	-98 155	346 660
27	135	143 479	-96 476	426 375
28	140	144 935	-95 322	504 206
29	145	146 147	-94 472	579 661
30	150	147 172	-93 816	652 369
31	155	148 051	-93 289	721 758
32	160	148 810	-92 853	787 641
33	165	149 468	-92 482	849 616
34	170	150 020	-92 160	907 365
35	175	150 534	-91 875	960 593
36	180	150 961	-91 619	1069 130
37	185	151 327	-91 385	1052 420
38	190	151 636	-91 169	1090 572
39	195	151 893	-90 467	1123 265
40	200	152 100	-90 724	1156 143
41	205	152 259	-90 590	1171 670
42	210	152 373	-90 412	1187 138
43	215	152 443	-90 237	1196 669
44	220	152 468	-90 064	1200 216
45	225	152 451	-89 892	1197 760
46	230	152 394	-89 718	1180 314
47	235	152 283	-89 540	1174 520
48	240	151 132	-89 357	1154 559
49	245	151 934	-89 167	1128 304
50	250	151 687	-89 966	1096 925
51	255	151 287	-88 753	1059 759
52	260	151 072	-88 523	1017 300
53	265	150 616	-88 271	969 761
54	270	150 134	-87 992	917 385
55	275	149 577	-87 678	860 436
56	280	148 936	-87 317	799 206

57	285	148 171	-86.874	734 008
58	290	147 342	-86.385	665 182
59	295	146 345	-65.756	573 086
60	300	145 172	-84.949	518 111
61	305	143 766	-93.863	440.673
62	310	142 040	-62.363	261 364
63	315	139 841	-79.853	280.460
64	320	126 868	-75.406	199 180
65	325	132 448	-64.943	119 738
66	330	125.878	-24.876	56 198
67	335	120 517	50 244	79 747
68	340	134 643	70.623	154 522
69	345	138 315	77.665	175 388
70	350	140 891	50 059	716 511
71	355	142 654	82 575	346 782
72	360	144 424	84 291	473 779
73	365	145 718	25 237	551 775
74	370	146 608	85.956	625 519
75	375	147 728	86.526	656 208
76	380	148 539	86.993	763 484
77	385	149.333	87.386	826 520
78	390	149 835	87.725	866 382
79	395	150 257	88 022	541 372
80	400	150 610	88 126	591 515
81	405	151 157	88 570	1076.518
82	410	151 557	88 752	1076 548
83	415	151 803	88 939	1111 548
84	420	152 028	89.155	1140 892
85	425	152 205	89 342	1164 382
86	430	152 338	89 522	1183 050
87	435	152 422	89 698	1193 806
88	440	152 464	89 871	1199 563
89	445	152 462	90 044	1199 279
90	450	152 417	90 317	1193 168
91	455	152 338	90 393	1160 990
92	460	152 154	90 574	1162 966
93	465	152 014	90 751	1139 006
94	470	151 785	90 958	1109 413
95	475	151 505	91 166	1074.375
96	480	151 173	91 389	1033 770
97	485	150 776	91 632	988 103
98	490	150 323	91 900	937 504
99	495	149 795	92 300	862 371
100	500	149 185	92 542	803 545

ADMITTANCE (-4 E-2,-2 E-2)

PRESSURE DISTRIBUTION

ITERATION	DISTANCE	MAG(dB)	PHASE	PRESSURE
0	0 000	152 467	-0 000	1200 000
1	005	152 433	-0 254	1195 309
2	010	152 355	-0 512	1184 653
3	015	152 233	-0 776	1168 086
4	020	152 064	-0 148	1145 692
5	025	151 849	-0 333	1117 584
6	030	151 583	-0 634	1083 917
7	035	151 264	-0 956	1044 030
8	040	150 868	-0 275	1000 555
9	045	150 449	-0 689	951 306
10	050	149 542	-0 116	897 339
11	055	149 358	-0 601	838 932
12	060	148 685	-0 416	776 391
13	065	147 909	-0 823	710 047
14	070	147 610	-0 525	640 261
15	075	145 961	-0 629	567 423
16	080	144 722	-0 736	491 509
17	085	143 231	-0 926	414 399
18	090	141 393	-0 232	335 346
19	095	139 039	-0 609	255 753
20	100	135 870	-1 14 669	172 557
21	105	131 485	-1 34 216	107 176
22	110	128 435	-1 73 850	75 436
23	115	132 423	-1 28 943	119 392
24	120	136 566	-1 12 749	192 372
25	125	139 546	-1 05 736	271 074
26	130	141 781	-1 01 856	350 686
27	135	143 543	-0 99 473	429 512
28	140	144 978	-0 77 797	506 717
29	145	146 177	-0 6 559	581 703
30	150	147 194	-0 5 600	653 984
31	155	148 068	-0 4 629	723 135
32	160	148 822	-0 4 189	788 772
33	165	149 477	-0 3 645	850 540
34	170	150 046	-0 3 173	905 113
35	175	150 539	-0 2 755	961 100
36	180	150 445	-0 1 379	1009 467
37	185	151 030	-0 0 056	1053 786
38	190	151 678	-0 1 718	1050 835
39	195	151 851	-0 1 321	1123 450
40	200	152 101	-0 1 178	1150 464
41	205	152 260	-0 0 868	1171 741
42	210	152 373	-0 0 605	1187 173
43	215	152 443	-0 0 349	1198 681
44	220	152 458	-0 0 195	1201 217
45	225	152 451	-0 0 941	1197 762
46	230	152 289	-0 0 585	1189 730
47	235	152 084	-0 0 224	1174 761
48	240	152 021	-0 0 655	1174 775
49	245	151 925	-0 0 372	1165 747
50	250	151 652	-0 0 190	1057 112
51	255	151 270	-0 0 187	1060 050
52	260	151 035	-0 0 139	1017 462
53	265	150 621	-0 0 497	770 273
54	270	150 140	-0 0 150	518 038
55	275	149 586	-0 0 568	861 256
56	280	148 947	-0 0 059	806 222

57	285	148	212	-65.439	715.258
58	290	147	362	-84.695	666.714
59	295	146	373	-83.775	594.968
60	300	145	210	-82.597	520.437
61	305	143	823	-81.016	443.593
62	310	142	129	-78.763	365.107
63	315	139	994	-75.259	325.468
64	320	137	177	-69.056	306.350
65	325	133	260	-55.500	171.616
66	330	128	740	-17.506	78.587
67	335	123	605	29.275	96.846
68	340	125	176	62.921	163.916
69	345	128	539	72.173	241.441
70	350	141	113	74.692	320.975
71	355	142	729	79.733	410.212
72	360	144	473	91.640	478.513
73	365	145	723	83.018	553.778
74	370	146	633	84.167	637.382
75	375	147	756	84.901	657.689
76	380	146	553	85.585	764.682
77	385	149	243	86.161	837.935
78	390	149	843	86.659	867.112
79	395	150	363	87.054	941.902
80	400	151	614	87.485	993.023
81	405	151	200	87.524	1027.214
82	410	151	520	98.166	1077.145
83	415	151	804	98.470	1111.911
84	420	152	129	85.758	1141.038
85	425	152	204	89.032	1164.470
86	430	152	376	89.197	1182.047
87	435	152	452	89.536	1193.825
88	440	152	464	89.811	1199.566
89	445	152	462	90.064	1199.380
90	450	152	417	91.314	1193.177
91	455	152	328	90.578	1181.031
92	460	152	154	90.844	1162.973
93	465	152	814	91.119	1129.123
94	470	151	786	91.418	1119.563
95	475	151	507	91.713	1074.933
96	480	151	174	92.042	1034.133
97	485	150	783	92.399	988.568
98	490	150	328	92.752	938.115
99	495	149	802	93.232	882.995
100	500	149	196	93.734	823.502

ADMITTANCE (2 E-2, 4 E-2)

PRESSURE DISTRIBUTION				
ITERATION	DISTANCE	MAG(db)	PHASE	PRESSURE
0	0 000	152 467	90 000	1000 000
1	005	152 470	90 010	1200 307
2	010	152 429	90 021	1194 759
3	015	152 344	90 031	1183 146
4	020	152 214	90 042	1165 604
5	025	152 018	90 053	1142 222
6	030	151 614	90 065	1113 118
7	035	151 539	90 077	1078 436
8	040	151 210	90 091	1038 351
9	045	150 623	90 105	993 064
10	050	150 372	90 121	942 801
11	055	149 850	90 139	887 814
12	060	149 248	90 159	828 379
13	065	148 554	90 182	764 794
14	070	147 752	90 210	697 377
15	075	146 831	90 244	626 467
16	080	145 728	90 287	552 417
17	085	144 428	90 344	475 601
18	090	142 646	90 423	396 412
19	095	140 895	90 542	315 218
20	100	138 210	90 745	232 457
21	105	134 320	91 177	148 537
22	110	126 994	92 745	63 904
23	115	117 485	-98 215	21 384
24	120	131 397	-91 640	106 097
25	125	136 478	-90 903	190 435
26	130	139 633	-90 617	273 831
27	135	141 909	-90 464	355 858
28	140	143 675	-90 369	476 104
29	145	145 105	-90 302	514 166
30	150	146 295	-90 253	589 652
31	155	147 303	-90 215	562 185
32	160	148 166	-90 184	731 399
33	165	148 912	-90 157	796 950
34	170	149 558	-90 137	858 507
35	175	150 137	-90 118	15 63
36	180	150 604	-90 101	98 431
37	185	151 023	-90 085	1016 247
38	190	151 381	-90 072	1058 971
39	195	151 882	-90 059	1006 320
40	200	151 922	-90 047	1128 345
41	205	152 132	-90 036	1154 536
42	210	152 284	-90 025	1175 074
43	215	152 392	-90 014	1189 673
44	220	152 434	-90 004	1198 312
45	225	153 474	-89 004	1200 947
46	230	153 440	-89 083	1397 565
47	235	153 381	-89 072	1198 187
48	240	152 168	-89 062	1177 844
49	245	152 101	-89 051	1151 813
50	250	151 013	-89 040	1124 854
51	255	151 148	-89 027	1152 117
52	260	151 341	-89 014	1153 946
53	265	150 975	-89 000	1010 520
54	270	150 549	-89 025	983 143
55	275	150 053	-89 068	908 895
56	280	149 483	-89 049	851 089
57	285	148 877	-89 067	888 216

51	205	148 025	-87 821	/87 018
58	290	148 166	-89 801	722 994
59	205	147 186	-89 769	653 348
60	300	146 158	-89 730	580 429
61	205	144 942	-89 679	504 602
62	310	143 476	-89 610	426 347
63	315	141 650	-89 509	345 758
64	210	139 300	-89 345	263 537
65	225	135 920	-89 032	180 001
66	210	131 490	-89 146	95 977
67	325	111 739	-73 906	11 036
68	340	128 310	87 656	74 438
69	345	134 912	88 913	159 010
70	350	138 588	88 209	242 609
71	355	141 131	88 487	325 396
72	360	143 161	89 610	406 356
73	365	144 603	89 676	485 280
74	371	145 674	89 730	541 774
75	375	146 945	89 773	635 453
76	380	147 659	89 805	705 049
77	385	148 646	89 832	772 908
78	391	149 327	89 855	825 994
79	393	149 618	89 875	894 892
80	401	150 431	89 913	949 107
81	405	150 874	89 916	998 965
82	410	151 234	89 923	1043 618
83	415	151 576	89 926	1063 042
84	420	151 844	89 948	1117 040
85	425	152 063	89 960	1145 441
86	426	152 103	89 971	1168 103
87	429	152 357	89 982	1184 912
88	440	152 436	89 992	1195 785
89	445	152 472	90 013	1210 666
90	450	152 462	90 015	1199 552
91	453	152 411	90 023	1192 388
92	460	152 315	90 034	1179 269
93	465	152 174	90 045	1160 342
94	470	151 986	90 056	1155 402
95	475	151 749	90 068	1114 873
96	480	151 461	90 081	1068 808
97	485	151 118	90 094	1027 388
98	490	150 715	90 109	980 821
99	495	150 247	90 125	926 340
100	500	149 115	90 144	873 202

ADMITTANCE (2 E-2, 2 E-2)

PRESSURE DISTRIBUTION

ITERATION	DISTANCE	MAG(dB)	PHASE	PRESSURE
0	0 000	152 467	0 000	1000 000
1	005	152 457	0 010	1198 600
2	010	152 404	0 021	1191 375
3	015	152 307	0 031	1178 060
4	020	152 164	0 042	1158 902
5	025	151 975	0 054	1133 709
6	030	151 736	0 066	1103 274
7	035	151 447	0 078	1067 031
8	040	151 102	0 092	1025 482
9	045	150 697	0 107	972 796
10	050	150 327	0 123	927 205
11	055	149 683	0 141	870 969
12	060	149 057	0 163	816 369
13	065	148 375	0 187	745 708
14	070	147 499	0 217	677 312
15	075	146 526	0 253	605 522
16	080	145 380	0 299	536 600
17	085	144 007	0 361	453 318
18	090	142 729	0 440	373 466
19	095	140 186	0 586	291 344
20	100	127 276	0 830	208 764
21	105	132 797	0 402	124 646
22	110	122 917	0 392	79 968
23	115	123 928	-93 875	45 210
24	120	133 154	-91 339	129 874
25	125	137 489	-90 604	213 940
26	130	140 337	-90 569	296 943
27	135	142 443	-90 437	378 460
28	140	144 102	-90 351	458 083
29	145	145 457	-90 290	535 411
30	150	146 590	-90 245	611 057
31	155	147 554	-90 209	681 647
32	160	148 782	-90 180	749 822
33	165	149 098	-90 155	214 240
34	170	149 719	-90 134	874 579
35	175	150 360	-90 116	30 125
36	180	150 724	-90 100	61 150
37	185	151 125	-90 065	1008 205
38	190	151 466	-90 071	1150 420
39	195	151 763	-90 055	1105 264
40	200	151 589	-90 047	1125 602
41	205	152 174	-90 036	1160 260
42	210	152 314	-90 025	1179 084
43	215	152 409	-90 014	1192 001
44	220	152 459	-90 004	1198 946
45	225	152 466	-89 554	1199 483
46	230	152 406	-89 582	1194 815
47	235	152 748	-89 571	1183 748
48	240	152 220	-89 582	1181 745
49	245	152 051	-89 551	1143 14
50	250	153 871	-89 535	1115 281
51	255	151 561	-89 527	1081 347
52	260	151 277	-89 513	1041 614
53	265	150 855	-89 509	996 326
54	270	150 410	-89 503	947 139
55	275	149 895	-89 506	892 506

56	280	149 301	-89 846	833 502
57	285	148 617	-69 823	770 322
58	290	147 826	-89 795	703 283
59	295	146 907	-89 762	632 720
60	300	145 831	-89 710	558 987
61	305	144 552	-89 664	482 454
62	310	143 100	-89 588	413 504
63	315	141 055	-89 473	133 534
64	320	128 486	-89 381	230 649
65	325	134 755	-89 864	156 169
66	330	127 985	-89 553	71 630
67	335	113 626	77 110	13 713
68	340	120 702	89 215	98 200
69	345	136 115	89 054	163 632
70	350	129 383	89 260	262 662
71	355	141 720	89 521	348 213
72	360	143 524	89 511	422 584
73	365	144 680	89 589	506 613
74	370	146 189	89 740	592 505
75	375	147 212	89 770	555 280
76	380	148 187	89 810	124 772
77	385	142 843	89 626	700 632
78	390	144 457	89 856	653 574
79	395	150 045	89 577	910 150
80	400	150 558	89 894	623 227
81	405	150 662	89 510	1011 469
82	410	151 213	89 524	1054 643
83	415	151 652	89 576	1052 577
84	420	151 506	89 549	1124 646
85	425	152 110	89 560	1151 728
86	430	152 287	89 571	1172 708
87	435	152 578	89 582	1187 571
88	440	152 445	89 592	1197 653
89	445	152 468	89 603	1210 227
90	450	152 448	89 613	1197 417
91	455	152 284	89 623	1188 579
92	460	152 375	89 634	1173 705
93	465	152 121	89 645	1153 130
94	470	151 510	89 657	1126 667
95	475	151 668	89 669	1054 559
96	480	151 385	89 681	1057 627
97	485	151 005	89 695	1014 159
98	490	151 585	89 551	106 210
99	495	151 145	89 127	917 450
100	500	149 577	89 145	958 887

ADMITTANCE (2 E-2, 0 E+0)

PRESSURE DISTRIBUTION

ITERATION	DISTANCE	MAG(dB)	PHASE	PRESSURE
0	0 000	152 467	90 000	1200 000
1	005	152 445	90 010	1196 904
2	010	152 379	90 021	1187 590
3	015	152 269	90 032	1173 035
4	020	152 114	90 043	1152 211
5	025	151 911	90 054	1125 595
6	030	151 658	90 066	1093 356
7	035	151 353	90 079	1055 626
8	040	150 992	90 093	1012 614
9	045	150 569	90 108	964 520
10	050	150 679	90 125	911 609
11	055	149 514	90 144	854 124
12	060	148 862	90 166	792 358
13	065	148 100	90 182	726 623
14	070	147 238	90 203	657 248
15	075	146 220	90 222	584 579
16	080	145 017	90 242	508 582
17	085	143 569	90 260	430 336
18	090	141 778	90 278	350 531
19	095	139 461	90 297	268 472
20	100	136 230	90 316	185 072
21	105	130 949	91 735	100 758
22	110	115 054	100 914	16 164
23	115	127 675	-92 534	60 116
24	120	134 614	-91 132	153 652
25	125	138 394	-90 724	237 445
26	130	140 988	-90 528	320 055
27	135	142 947	-90 412	401 062
28	140	144 509	-90 335	480 062
29	145	145 795	-90 279	556 656
30	150	146 876	-90 237	630 463
31	155	147 709	-90 203	701 110
32	160	148 593	-90 175	768 245
33	165	149 281	-90 152	831 531
34	170	149 877	-90 132	890 651
35	175	150 395	-90 114	945 308
36	180	150 942	-90 098	995 229
37	185	151 225	-90 080	1040 164
38	190	151 551	-90 071	1070 887
39	195	151 802	-90 058	1114 200
40	200	152 043	-90 047	1142 930
41	205	152 517	-90 036	1185 734
42	210	152 343	-90 025	1183 096
43	215	152 423	-90 014	1194 330
44	220	152 464	-90 004	1195 581
45	225	152 498	-89 994	1198 521
46	230	152 409	-89 980	1192 044
47	235	152 318	-89 970	1179 215
48	240	152 157	-89 962	1160 657
49	245	151 093	-89 950	1152 055
50	250	151 760	-89 938	1146 049
51	255	151 474	-89 921	1070 254
52	260	151 324	-89 910	1027 043
53	265	150 735	-89 898	493 074
54	270	150 171	-89 881	431 031
55	275	149 704	-89 863	876 110
56	280	149 116	-89 842	815 717
57	--	--	--	--

57	285	148 403	-87 818	/51.528
58	290	147 579	-89 789	683 573
59	295	146 619	-89 754	612 093
60	300	145 491	-89 708	537 547
61	305	144 144	-89 648	460 307
62	310	142 496	-89 563	280 762
63	315	140 406	-89 433	299 311
64	320	137 587	-89 203	216 363
65	325	133 317	-88 603	132 338
66	330	124 453	-86 324	47 700
67	335	122 355	85 316	37 463
68	340	132 619	88 571	122.129
69	345	137 171	89 162	206 254
70	350	140 112	87 412	287 335
71	355	142 371	89 550	271 009
72	360	143 567	87 639	450 006
73	365	145 241	89 702	528 345
74	370	146 493	89 749	603 337
75	375	147 471	89 725	675 187
76	380	148 210	89 615	743 594
77	385	149 035	89 840	808 357
78	390	149 664	89 861	869 069
79	395	150 210	89 279	925 427
80	400	150 682	89 846	977 146
81	405	151 089	89 611	1023 574
82	410	151 476	89 524	1065 549
83	415	151 727	89 937	1102 024
84	420	151 967	89 549	1131 859
85	425	152 157	89 960	1158 017
86	430	152 211	89 971	1177 273
87	435	152 400	89 982	1190 830
88	440	152 455	89 992	1198 221
89	445	152 466	90 003	1166 508
90	450	152 433	90 113	1195 283
91	455	152 356	90 323	1164 770
92	460	152 234	90 124	1163 331
93	465	152 067	90 045	1146 018
94	470	151 852	90 057	1117 573
95	475	151 586	90 069	1084 326
96	480	151 267	90 082	1045 248
97	485	150 891	90 097	1000 031
98	490	150 452	90 112	931 600
99	495	149 944	90 130	267 501
100	500	149 257	90 149	838 916

ADMITTANCE = (2.E-2,-2 E-2)

PRESSURE DISTRIBUTION				
ITERATION	DISTANCE	MAG(db)	PHASE	PRESSURE
0	0 000	152 467	90 000	1000 000
1	005	152 433	90 010	1195 297
2	010	152 355	90 021	1184 606
3	015	152 232	90 032	1167 570
4	020	152 063	90 043	1145 500
5	025	151 846	90 054	1117 382
6	030	151 579	90 067	1083 467
7	035	151 259	90 080	1044 322
8	040	150 881	90 094	1009 746
9	045	150 440	90 110	950 261
10	050	149 929	90 127	896 614
11	055	149 341	90 147	837 279
12	060	148 663	90 170	774 348
13	065	147 878	90 197	707 538
14	070	146 968	90 220	637 183
15	075	145 903	90 272	563 636
16	080	144 638	90 326	487 265
17	085	143 106	90 401	408 453
18	090	141 190	90 512	337 596
19	095	138 670	90 697	245 100
20	100	135 640	91 074	161 380
21	105	128 599	92 274	76 875
22	110	109 640	-110 678	8 667
23	115	130 257	-91 882	93 041
24	120	135 264	-90 980	177 433
25	125	139 214	-90 659	260 952
26	130	141 593	-90 493	343 167
27	135	143 424	-90 390	423 665
28	140	144 898	-90 320	502 041
29	145	146 120	-90 269	577 902
30	150	147 153	-90 229	650 868
31	155	148 037	-90 198	720 573
32	160	148 799	-90 171	786 668
33	165	149 459	-90 149	848 822
34	170	150 033	-90 130	906 733
35	175	150 529	-90 113	960 081
36	180	150 959	-90 097	1008 628
37	185	151 324	-90 083	1052 123
38	190	151 634	-90 070	1090 745
39	195	151 892	-90 058	1123 105
40	200	152 099	-90 046	1150 239
41	205	152 259	-90 035	1171 607
42	210	152 373	-90 125	1187 107
43	215	152 443	-90 014	1196 658
44	220	152 468	-90 004	1200 215
45	225	152 450	-89 994	1197 257
46	230	152 389	-89 982	1189 299
47	235	152 287	-89 972	1174 682
48	240	152 133	-89 961	1154 578
49	245	151 932	-89 950	1128 480
50	250	151 885	-89 938	1096 745
51	255	151 385	-89 925	1059 105
52	260	151 015	-89 911	1018 952
53	265	150 512	-89 896	973 321
54	270	150 129	-89 880	936 823
55	275	149 570	-89 861	859 721
56	280	148 927	-89 839	798 332
57	---	---	---	---

57	265	148 184	-82 813	732 733
58	290	147 325	-89 703	663 862
59	295	146 322	-89 745	591 466
60	200	145 138	-89 696	516 106
61	305	143 716	-89 630	438 160
62	310	141 661	-89 535	350 130
63	215	139 704	-89 385	276 088
64	320	136 584	-89 165	192 777
65	225	133 593	-88 193	108 310
66	330	118 428	-82 208	23 838
67	335	126 644	87 143	61 364
68	340	134 165	82 805	145 580
69	345	138 113	82 248	229 877
70	250	120 764	82 476	312 622
71	355	142 769	89 576	593 815
72	260	144 281	87 656	473 171
73	365	145 689	82 714	566 277
74	270	146 785	82 757	623 669
75	375	147 722	89 761	564 573
76	380	148 537	89 819	762 417
77	385	146 224	89 643	826 081
78	390	149 818	89 863	865 510
79	245	150 352	89 881	540 544
80	400	151 805	89 867	951 140
81	405	151 165	82 532	1026 478
82	410	151 525	89 525	1174 254
83	415	151 611	82 532	1111 516
84	420	152 117	82 548	1146 728
85	425	152 304	82 581	1164 305
86	430	152 335	82 571	1183 619
87	435	152 423	89 982	1193 790
88	440	153 464	82 992	1190 590
89	445	153 462	80 803	1160 570
90	450	153 417	80 123	1152 120
91	455	153 328	80 024	1160 562
92	460	153 144	80 124	1152 847
93	465	152 013	80 046	1138 906
94	470	151 784	80 057	1116 285
95	475	151 504	80 070	1074 054
96	480	151 160	80 083	1032 468
97	485	150 770	80 098	987 703
98	490	150 319	80 114	936 590
99	495	149 788	80 102	869 583
00	500	149 178	80 153	820 758

ADMITTANCE = (2 E-2,-4 E-2)

PRESSURE DISTRIBUTION

ITERATION	DISTANCE	MAG (db)	PHASE	PRESSURE
0	0 000	152 467	90 000	1200 000
1	005	152 420	90 010	1193 601
2	010	152 330	90 021	1181 232
3	015	152 194	90 032	1162 924
4	020	152 012	90 043	1139 797
5	025	151 721	90 055	1108 669
6	030	151 500	90 067	1073 583
7	035	151 164	90 081	1032 818
8	040	150 768	90 095	986 878
9	045	150 309	90 111	925 993
10	050	149 777	90 130	880 419
11	055	149 164	90 150	820 434
12	060	148 457	90 174	756 338
13	065	147 641	90 203	688 453
14	070	146 690	90 238	617 118
15	075	145 574	90 262	542 652
16	080	144 242	90 341	463 548
17	085	143 616	90 424	386 071
18	090	140 559	90 551	304 661
19	095	137 799	90 771	221 728
20	100	133 661	91 258	137 691
21	105	125 369	93 399	53 005
22	110	121 649	-95 448	32 234
23	115	132 245	-91 497	116 972
24	120	136 956	-90 664	201 214
25	125	139 963	-90 604	284 458
26	130	142 159	-90 461	366 279
27	135	143 875	-90 370	446 267
28	140	145 270	-90 307	524 019
29	145	146 434	-90 259	599 147
30	150	147 421	-90 222	671 273
31	155	148 268	-90 192	740 036
32	160	149 000	-90 167	805 091
33	165	149 635	-90 146	866 113
34	170	150 185	-90 127	922 795
35	175	150 662	-90 111	974 293
36	180	151 172	-90 046	1022 028
37	185	151 433	-90 082	1064 082
38	190	151 717	-90 059	1100 804
39	195	151 960	-90 053	1132 011
40	200	155 154	-90 046	1157 546
41	205	152 301	-90 035	1177 282
42	210	152 402	-90 025	1191 119
43	215	152 459	-90 014	1198 798
44	220	152 473	-90 004	1200 850
45	225	152 441	-90 003	1196 675
46	230	152 379	-89 983	1086 544
47	235	152 150	-89 972	1170 144
48	240	151 086	-89 961	1148 496
49	245	151 873	-89 950	1120 75
50	250	151 611	-89 937	1087 445
51	255	151 395	-89 930	1048 457
52	260	150 923	-89 910	1004 625
53	265	150 488	-89 895	955 569
54	270	149 984	-89 877	901 716
55	275	149 403	-89 858	843 344
56	280	149 227	-89 837	811 117

50	280	148 133	-82 835	80 748
52	285	147 960	-89 809	714 240
58	290	147 663	-89 776	244 153
59	295	146 613	-89 736	570 839
60	300	144 769	-89 683	454 666
61	305	143 365	-89 611	416 614
62	310	141 361	-89 504	335 279
63	315	138 541	-89 320	152 867
64	320	135 481	-89 980	369 193
65	325	129 230	-87 531	84 627
66	330	100 641	6 633	3 175
67	335	127 505	87 748	69 333
68	340	125 463	86 973	169 873
69	345	122 563	89 318	163 466
70	350	141 417	89 593	215 901
71	355	142 276	89 600	415 221
72	360	144 750	89 572	155 255
73	365	146 822	89 724	871 406
74	370	147 870	89 765	244 857
75	375	147 566	89 727	714 760
76	380	142 739	89 824	781 239
77	385	149 408	89 846	843 865
78	390	149 589	89 656	112 142
79	395	150 493	89 583	993 561
80	400	150 500	89 819	1014 587
81	405	151 296	89 513	1148 562
82	410	151 513	89 616	1157 516
83	415	151 675	89 538	1121 302
84	420	152 167	89 681	1148 671
85	425	152 251	89 581	1170 563
86	430	152 570	89 571	1186 644
87	435	152 442	89 482	1195 740
88	440	151 471	89 662	1210 856
89	445	152 459	89 603	1198 650
90	450	152 413	89 613	1151 675
91	455	152 300	89 624	1177 153
92	460	152 153	89 635	1157 773
93	465	151 452	89 646	1171 594
94	470	151 715	89 158	1100 544
95	475	151 420	89 171	1183 781
96	480	151 169	89 184	1121 687
97	485	150 859	89 190	114 475
98	490	150 389	89 126	122 287
99	495	149 570	89 174	855 664
100	500	148 555	89 176	114 510

Computer Hardware and Software

The data reduction program was coded in FORTRAN 77 using a HP-3000 system. The perturbation pressure graphs were done with the Lotus 123 software on an IBM clone with a Gemini 10x printer.

* Page 62 does not exist